The Abdus Salam
International Centre for Theoretical Physics

United Nations
Educational, Scientific
and Cultural Organization

International Atomic
Energy Agency

SMR.1771 - 9

Conference and Euromech Colloquium #480

on

High Rayleigh Number Convection

4 - 8 Sept., 2006, ICTP, Trieste, Italy

Local heat transport analysis based on DNS/LES of turbulent RBC in wide containers

O. Shishkina
DLR-Institute of Aerodynamics & Flow Technology
Goettingen
Germany

Strada Costiera 11, 34014 Trieste, Italy - Tel. +39 040 2240 111; Fax +39 040 224 163 - sci_info@ictp.it, www.ictp.it

Local heat transport analysis based on DNS/LES of turbulent RBC in wide cylindrical containers

Olga Shishkina & Claus Wagner

German Aerospace Center
Institute for Aerodynamics and Flow Technology
Göttingen

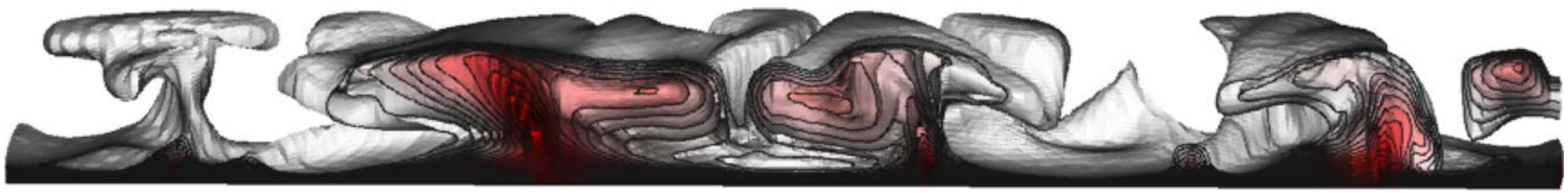

Outline

1. DNS and LES of turbulent Rayleigh–Bénard convection in wide cylindrical containers
2. Dependences of the flow patterns on Ra and Γ
3. Thermal plume extraction
4. Thermal dissipation rate analysis
5. Spatial distribution of the local heat fluxes

DLR

Outline

1. DNS and LES of turbulent Rayleigh–Bénard convection in wide cylindrical containers
2. Dependences of the flow patterns on Ra and Γ
3. Thermal plume extraction
4. Thermal dissipation rate analysis
5. Spatial distribution of the local heat fluxes

Conducted DNS and LES of turbulent RBC in wide cylindrical containers

Main parameters

- Rayleigh number $Ra = \alpha g H^3 \Delta\theta / (\kappa\nu)$
- Prandtl number $Pr = \nu/\kappa$
- Aspect ratio $\Gamma = D/H$

Conducted simulations

- $Ra = 10^5, ..., 10^9$
- $Pr = 0.7$
- $\Gamma = 10, \Gamma = 5$

H height of the cylinder
D diameter of the cylinder
κ thermal diffusivity
ν kinematic viscosity
$\Delta\theta$ temperature difference
α thermal expansion coefficient
g gravitational acceleration

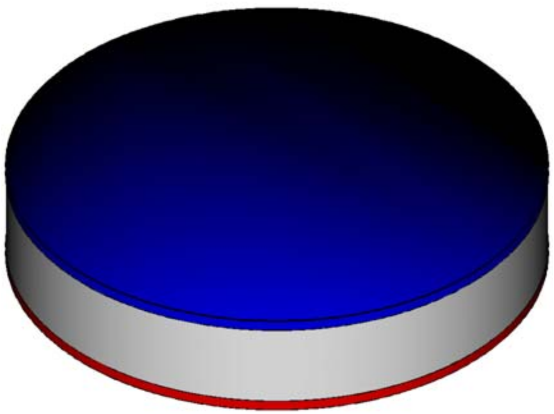

Conducted DNS and LES of turbulent RBC in wide cylindrical containers

Main parameters

- Rayleigh number $Ra = \alpha g H^3 \Delta\theta / (\kappa\nu)$
- Prandtl number $Pr = \nu/\kappa$
- Aspect ratio $\Gamma = D/H$

Conducted simulations

- $Ra = 10^5, ..., 10^9$
- $Pr = 0.7$
- $\Gamma = 10, \Gamma = 5$

H height of the cylinder
D diameter of the cylinder
κ thermal diffusivity
ν kinematic viscosity
$\Delta\theta$ temperature difference
α thermal expansion coefficient
g gravitational acceleration

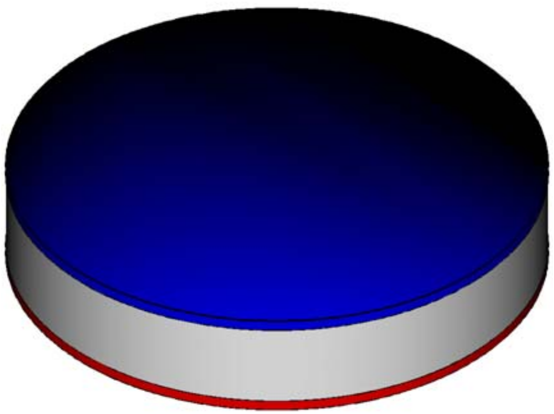

Conducted DNS and LES of turbulent RBC in wide cylindrical containers

Main parameters

- Rayleigh number $Ra = \alpha g H^3 \Delta\theta/(\kappa\nu)$
- Prandtl number $Pr = \nu/\kappa$
- Aspect ratio $\Gamma = D/H$

Conducted simulations

- $Ra = 10^5, ..., 10^9$
- $Pr = 0.7$
- $\Gamma = 10, \Gamma = 5$

H height of the cylinder
D diameter of the cylinder
κ thermal diffusivity
ν kinematic viscosity
$\Delta\theta$ temperature difference
α thermal expansion coefficient
g gravitational acceleration

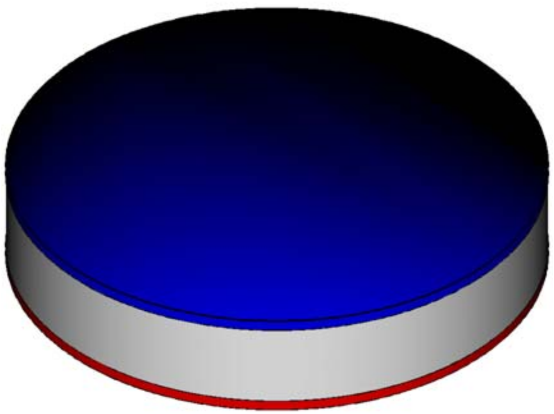

Finite volume approach to simulation of RBC

Filtered governing dimensionless equations

$$\frac{\partial \overline{u}_i}{\partial t} + \frac{\partial(\overline{u}_i\overline{u}_j)}{\partial x_j} + \frac{\partial \tau_{ij}}{\partial x_j} + \frac{\partial \overline{p}}{\partial x_i} = 2\left(\frac{Pr}{\Gamma^3 Ra}\right)^{1/2}\frac{\partial \overline{S}_{ij}}{\partial x_j} + \overline{T}\delta_{i3}$$

$$\frac{\partial \overline{u}_i}{\partial x_i} = 0$$

$$\frac{\partial \overline{T}}{\partial t} + \frac{\partial(\overline{T}\overline{u}_j)}{\partial x_j} + \frac{\partial \tau_{Tj}}{\partial x_j} = \left(\frac{1}{\Gamma^3 RaPr}\right)^{1/2}\frac{\partial^2 \overline{T}}{\partial x_j^2}$$

Filtered strain tensor

$$\overline{S}_{ij} = \frac{1}{2}\left(\frac{\partial \overline{u}_i}{\partial x_j} + \frac{\partial \overline{u}_j}{\partial x_i}\right)$$

Subgrid scale stress tensors

$$\tau_{ij} = \overline{u_i u_j} - \overline{u}_i\overline{u}_j$$

$$\tau_{Tj} = \overline{Tu_j} - \overline{T}\,\overline{u}_j$$

Finite volume approach to simulation of RBC

Filtered governing dimensionless equations

$$\frac{\partial \overline{u}_i}{\partial t} + \frac{\partial(\overline{u}_i \overline{u}_j)}{\partial x_j} + \frac{\partial \tau_{ij}}{\partial x_j} + \frac{\partial \overline{p}}{\partial x_i} = 2\left(\frac{Pr}{\Gamma^3 Ra}\right)^{1/2} \frac{\partial \overline{S}_{ij}}{\partial x_j} + \overline{T}\delta_{i3}$$

$$\frac{\partial \overline{u}_i}{\partial x_i} = 0$$

$$\frac{\partial \overline{T}}{\partial t} + \frac{\partial(\overline{T}\overline{u}_j)}{\partial x_j} + \frac{\partial \tau_{Tj}}{\partial x_j} = \left(\frac{1}{\Gamma^3 RaPr}\right)^{1/2} \frac{\partial^2 \overline{T}}{\partial x_j^2}$$

Filtered strain tensor

$$\overline{S}_{ij} = \frac{1}{2}\left(\frac{\partial \overline{u}_i}{\partial x_j} + \frac{\partial \overline{u}_j}{\partial x_i}\right)$$

Subgrid scale stress tensors

$$\tau_{ij} = \overline{u_i u_j} - \overline{u}_i \overline{u}_j$$

$$\tau_{Tj} = \overline{T u_j} - \overline{T}\,\overline{u}_j$$

DLR

Finite volume approach to simulation of RBC

Filtered governing dimensionless equations

$$\frac{\partial \overline{u}_i}{\partial t} + \frac{\partial(\overline{u}_i \overline{u}_j)}{\partial x_j} + \frac{\partial \tau_{ij}}{\partial x_j} + \frac{\partial \overline{p}}{\partial x_i} = 2\left(\frac{Pr}{\Gamma^3 Ra}\right)^{1/2} \frac{\partial \overline{S}_{ij}}{\partial x_j} + \overline{T}\delta_{i3}$$

$$\frac{\partial \overline{u}_i}{\partial x_i} = 0$$

$$\frac{\partial \overline{T}}{\partial t} + \frac{\partial(\overline{T}\overline{u}_j)}{\partial x_j} + \frac{\partial \tau_{Tj}}{\partial x_j} = \left(\frac{1}{\Gamma^3 Ra Pr}\right)^{1/2} \frac{\partial^2 \overline{T}}{\partial x_j^2}$$

Filtered strain tensor

$$\overline{S}_{ij} = \frac{1}{2}\left(\frac{\partial \overline{u}_i}{\partial x_j} + \frac{\partial \overline{u}_j}{\partial x_i}\right)$$

Subgrid scale stress tensors

$$\tau_{ij} = \overline{u_i u_j} - \overline{u}_i \overline{u}_j$$

$$\tau_{Tj} = \overline{T u_j} - \overline{T}\,\overline{u}_j$$

LES: Tensor diffusivity subgrid-scale model

Exact series expansions for subgrid scale stress tensors

$$\overline{uv} - \overline{u}\,\overline{v} = \frac{1}{12} \sum_{\beta=z,r,\varphi} \Delta\beta^2 \frac{\partial \overline{u}}{\partial \beta} \frac{\partial \overline{v}}{\partial \beta} + \mathcal{O}\left(\sum_{\beta=z,r,\varphi} \Delta\beta^4 \right)$$

Leonard, Adv. Geophys. **18** (1974) 237

DNS: $10^5 \leq Ra \leq 10^7$

$$\overline{uv} - \overline{u}\,\overline{v} := 0$$

LES: Tensor diffusivity subgrid-scale model

Exact series expansions for subgrid scale stress tensors

$$\overline{uv} - \overline{u}\,\overline{v} = \frac{1}{12} \sum_{\beta=z,r,\varphi} \Delta\beta^2 \frac{\partial \overline{u}}{\partial \beta} \frac{\partial \overline{v}}{\partial \beta} + \mathcal{O}\left(\sum_{\beta=z,r,\varphi} \Delta\beta^4 \right)$$

DNS: $10^5 \leq Ra \leq 10^7$

$$\overline{uv} - \overline{u}\,\overline{v} := 0$$

LES: $10^8 \leq Ra \leq 10^9$

$$\overline{uv} - \overline{u}\,\overline{v} := \frac{1}{12} \sum_{\beta=z,r,\varphi} \Delta\beta^2 \frac{\partial \overline{u}}{\partial \beta} \frac{\partial \overline{v}}{\partial \beta}$$

LES: Tensor diffusivity subgrid-scale model

Exact series expansions for subgrid scale stress tensors

$$\overline{uv} - \overline{u}\,\overline{v} = \frac{1}{12} \sum_{\beta=z,r,\varphi} \Delta\beta^2 \frac{\partial \overline{u}}{\partial \beta} \frac{\partial \overline{v}}{\partial \beta} + \mathcal{O}\left(\sum_{\beta=z,r,\varphi} \Delta\beta^4 \right)$$

DNS: $10^5 \leq Ra \leq 10^7$

$$\overline{uv} - \overline{u}\,\overline{v} := 0$$

LES: $10^8 \leq Ra \leq 10^9$

$$\overline{uv} - \overline{u}\,\overline{v} \quad := \quad \frac{1}{12} \sum_{\beta=z,r,\varphi} \Delta\beta^2 \frac{\partial \overline{u}}{\partial \beta} \frac{\partial \overline{v}}{\partial \beta}$$

Numerical method

- fourth order spatial discretization schemes
- calculation of the velocity field at the cylinder axis
- hybrid explicit/semi-implicit time stepping
- numerical von Neumann stability
- adaptive mesh generation

Shishkina & Wagner *Computers & Fluids* (2006)
A fourth order finite volume scheme for turbulent flow simulations in cylindrical domains

Resolution check

$$Nu_{S_z} = \Gamma^{1/2} Ra^{1/2} Pr^{1/2} \langle u_z T \rangle_{t,S_z} - \Gamma^{-1} \langle \partial T / \partial z \rangle_{t,S_z}$$

$$Nu_V = \Gamma^{1/2} Ra^{1/2} Pr^{1/2} < u_z T >_{t,V} + 1$$

Nusselt numbers calculated at different locations, $\Gamma = 5$

Ra	10^6	10^7	10^8
Nu_{S_z} for $z = 0$	8.06	15.54	33.0
Nu_{S_z} for $z = H/2$	8.27	15.56	33.1
Nu_{S_z} for $z = H$	8.09	15.54	32.9
Nu_V	8.22	15.55	32.8
Mean Nu	8.2	15.55	32.9
Error, less than	1.7%	0.1%	0.7%
Time	42	107	43

Resolution check

$$Nu_{S_z} = \Gamma^{1/2} Ra^{1/2} Pr^{1/2} \langle u_z T \rangle_{t,S_z} - \Gamma^{-1} \langle \partial T / \partial z \rangle_{t,S_z}$$

$$Nu_V = \Gamma^{1/2} Ra^{1/2} Pr^{1/2} < u_z T >_{t,V} + 1$$

Nusselt numbers calculated at different locations, $\Gamma = 5$

Ra	10^6	10^7	10^8
Nu_{S_z} for $z = 0$	8.06	15.54	33.0
Nu_{S_z} for $z = H/2$	8.27	15.56	33.1
Nu_{S_z} for $z = H$	8.09	15.54	32.9
Nu_V	8.22	15.55	32.8
Mean Nu	8.2	15.55	32.9
Error, less than	1.7%	0.1%	0.7%
Time	42	107	43

Nusselt number vs. Rayleigh number

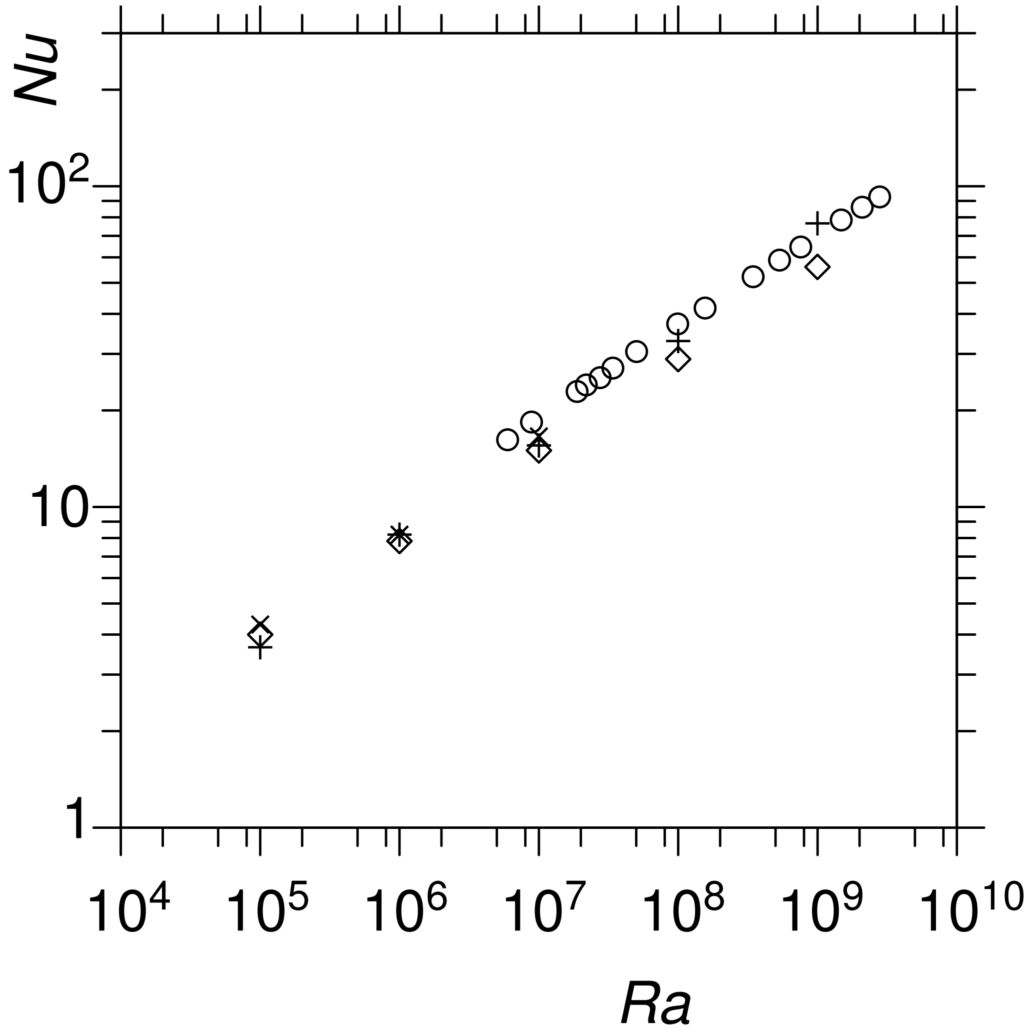

$Pr = 0.7, \Gamma = 5$ (pluses)

$Pr = 0.7, \Gamma = 10$ (crosses)

Shishkina & Wagner *J. Fluid Mech.* **546** (2006)

$Pr = 0.7, \Gamma = 6.7$ (diamonds)

Wu & Libchaber *Phys. Rev. A* **45** (1992)

$Pr = 0.68, \Gamma = 1$ (circles)

Niemela & Sreenivasan *J. Fluid Mech.* **481** (2003)

Outline

Mean temperature patterns at $z = H/2$, $Ra = 10^7$

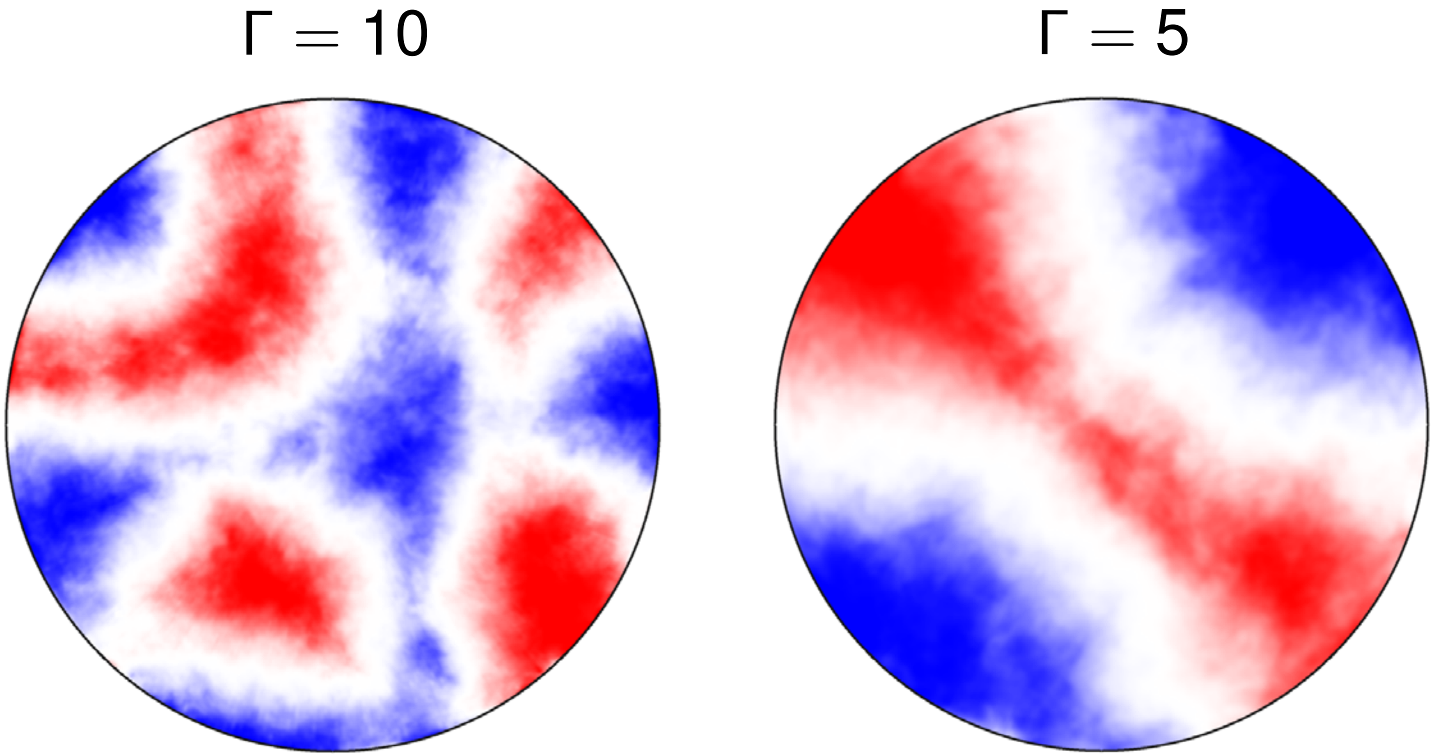

The colour scale ranges from blue (negative values) through white (zero) to red (positive values)

Mean flow structures depend strongly on the aspect ratio

Temperature patterns at $z = H/2$

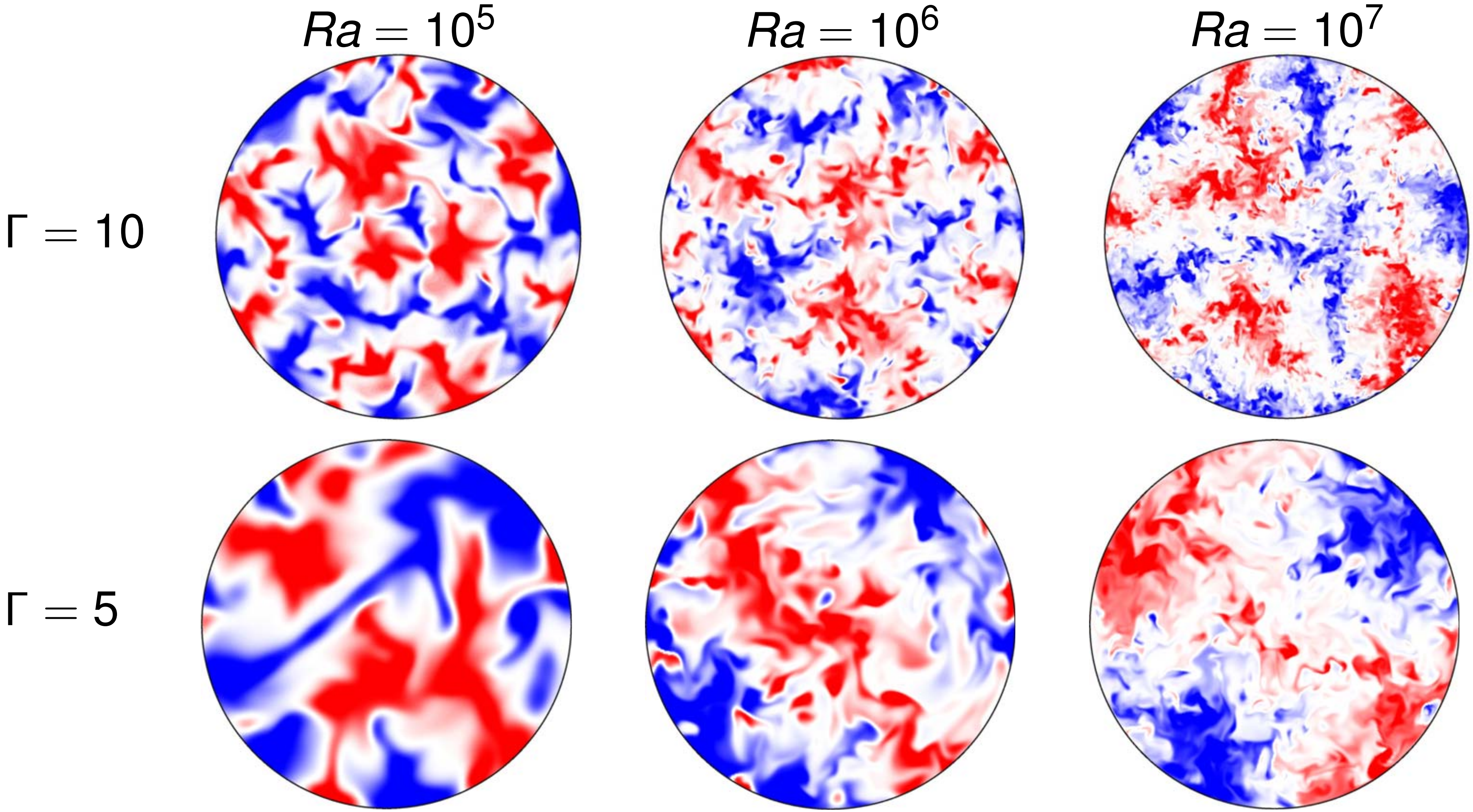

The number of visible large flow structures increases with Γ and decreases with growing Ra

Temperature patterns at $z = H/(2Nu)$

$Ra = 10^5$ | $Ra = 10^6$ | $Ra = 10^7$

$\Gamma = 10$

$\Gamma = 5$

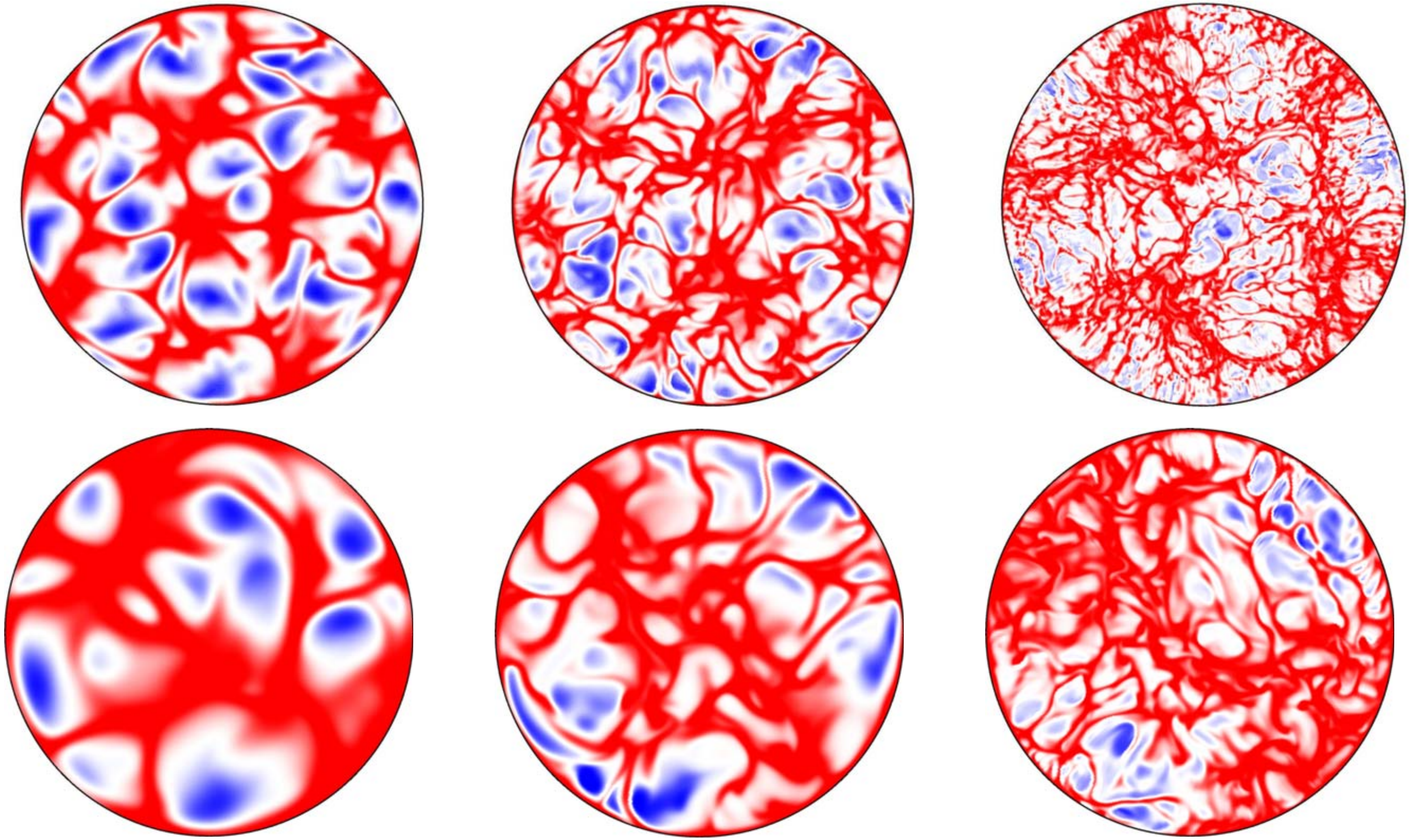

The plume roots become thinner with growing Ra and Γ

Vertical cross-sections of the temperature

for $Ra = 10^5$, $Pr = 0.7$, $\Gamma = 10$

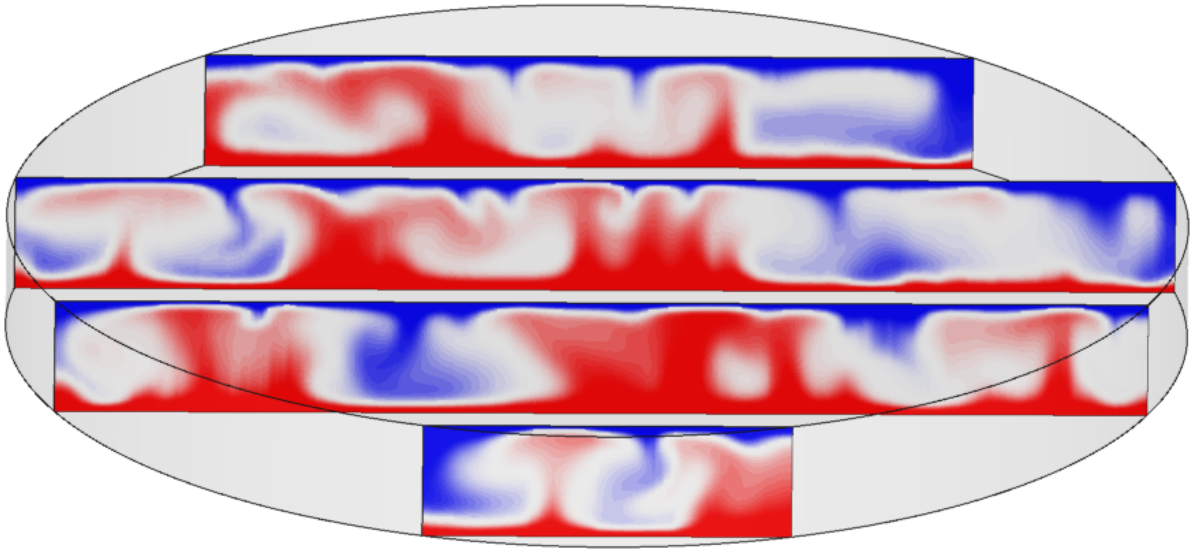

The colour scale ranges from blue (negative values) through white (zero) to red (positive values)

Warm and cold thermal plumes are seen in a mushroom-like form

Outline

Snapshots of $T\varepsilon_\theta$ in horizontal cross-sections

with superimposed velocity vectors for $Ra = 10^5$

Definition of $C(T, \varepsilon_\theta)$

$$C(T, \varepsilon_\theta) \equiv T\varepsilon_\theta$$

with the thermal dissipation rate

$$\varepsilon_\theta = \Gamma^{-3/2} Ra^{-1/2} Pr^{-1/2} (\nabla T)^2$$

Snapshots of $T\varepsilon_\theta$ in horizontal cross-sections

with superimposed velocity vectors for $Ra = 10^5$

$z = 10^{-2}H$

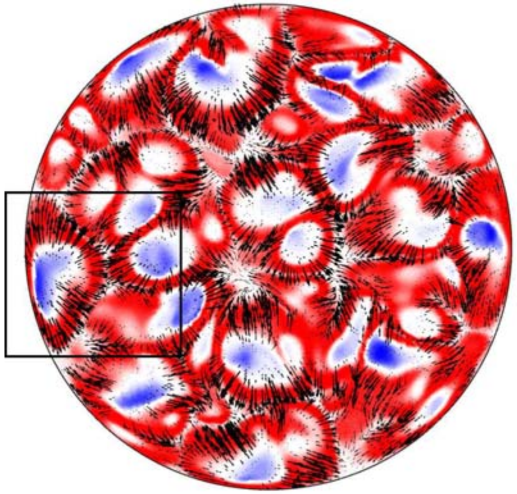

Snapshots of $T\varepsilon_\theta$ in horizontal cross-sections

with superimposed velocity vectors for $Ra = 10^5$

$z = 10^{-2} H$

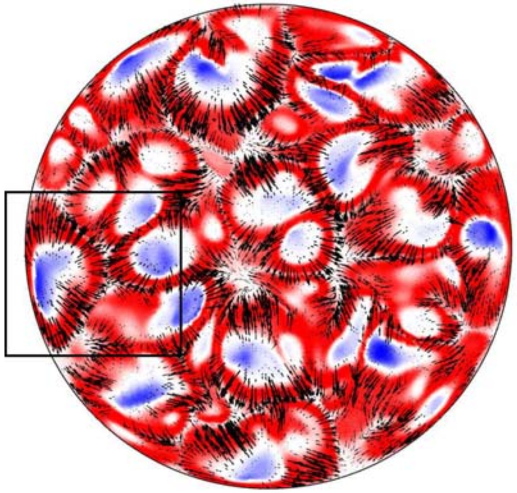

$z = H/(2Nu)$

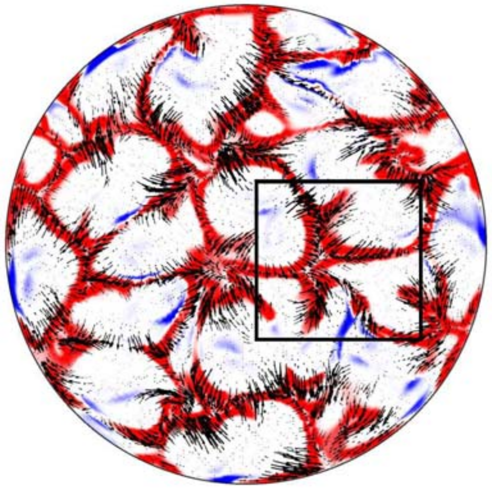

Snapshots of $T\varepsilon_\theta$ in horizontal cross-sections

with superimposed velocity vectors for $Ra = 10^5$

$z = 10^{-2}H$

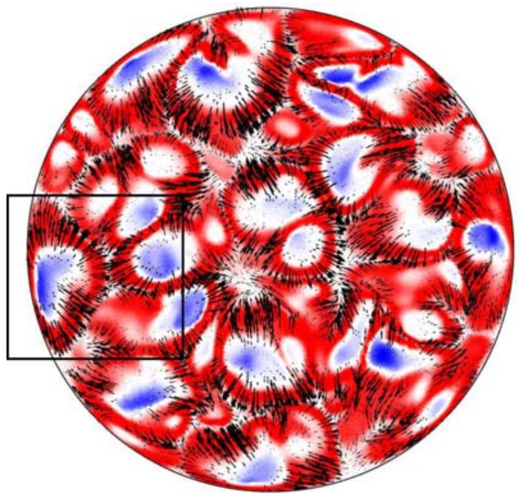

$z = H/(2Nu)$

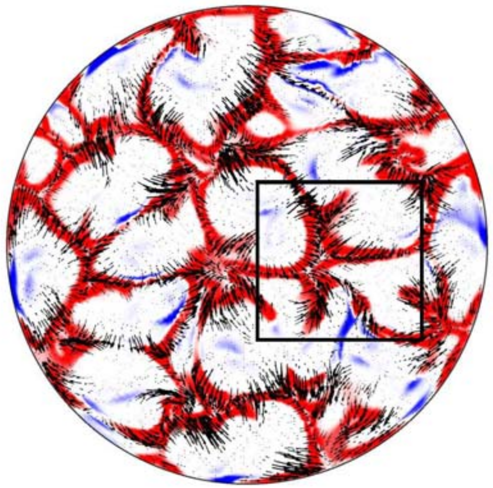

$z = H/2$

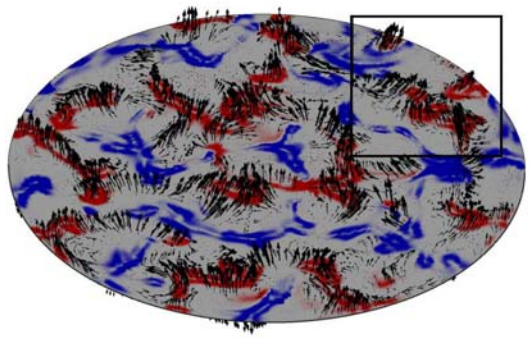

Snapshots of $T\varepsilon_\theta$ in horizontal cross-sections

with superimposed velocity vectors for $Ra = 10^5$

$z = 10^{-2}H$ $\qquad$ $z = H/(2Nu)$ $\qquad$ $z = H/2$

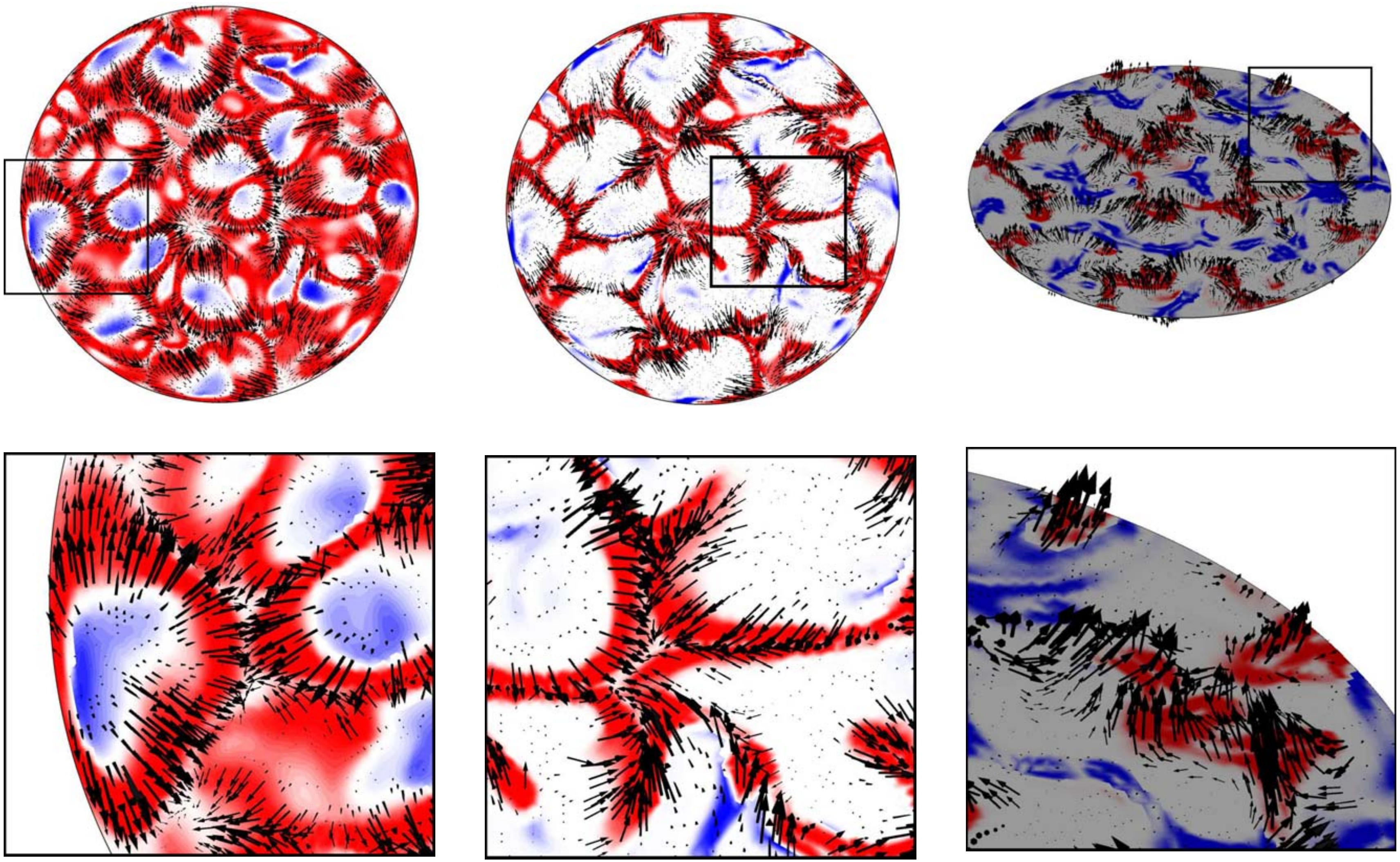

highlight the three-dimensional nature of the plumes

Structure sketch of a warm plume in the bulk

Superimposed instantaneous fields of $T\varepsilon_\theta$, $Ra = 10^5$, $z = \lambda_\theta$ (red) and $z = H - \lambda_\theta$ (blue)

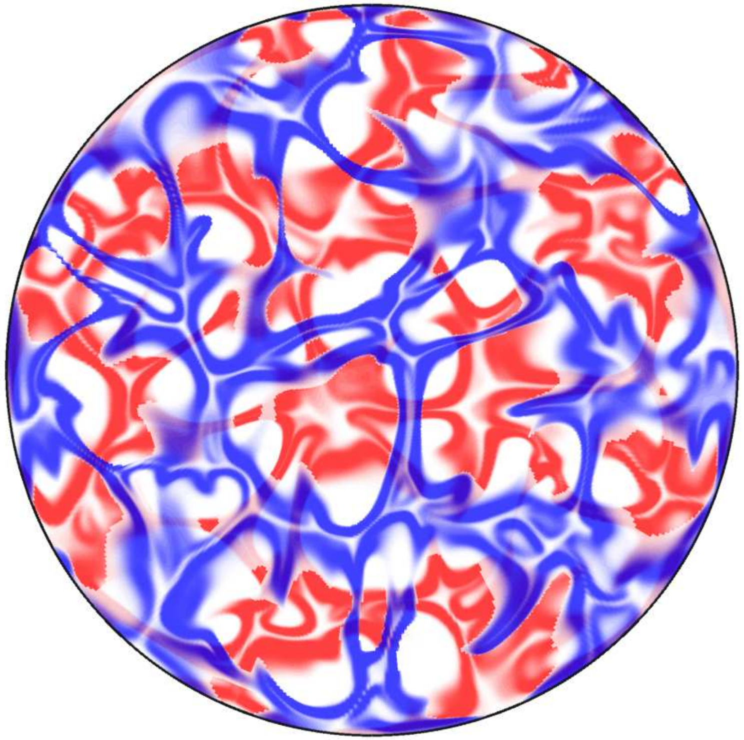

Superimposed instantaneous fields of $T\varepsilon_\theta$, $Ra = 10^5$, $z = \lambda_\theta$ (red) and $z = H - \lambda_\theta$ (blue)

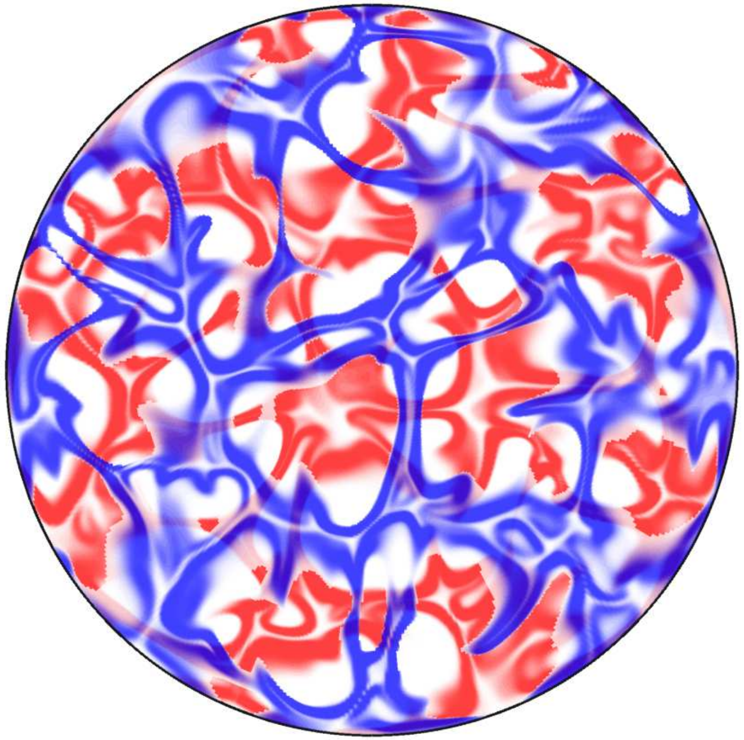

In moderate-Rayleigh-number case the roots of the warm and cold thermal plumes have a tendency to intersect at right angles.

Formation of warm and cold plumes in wide containers in moderate-Rayleigh-number regime

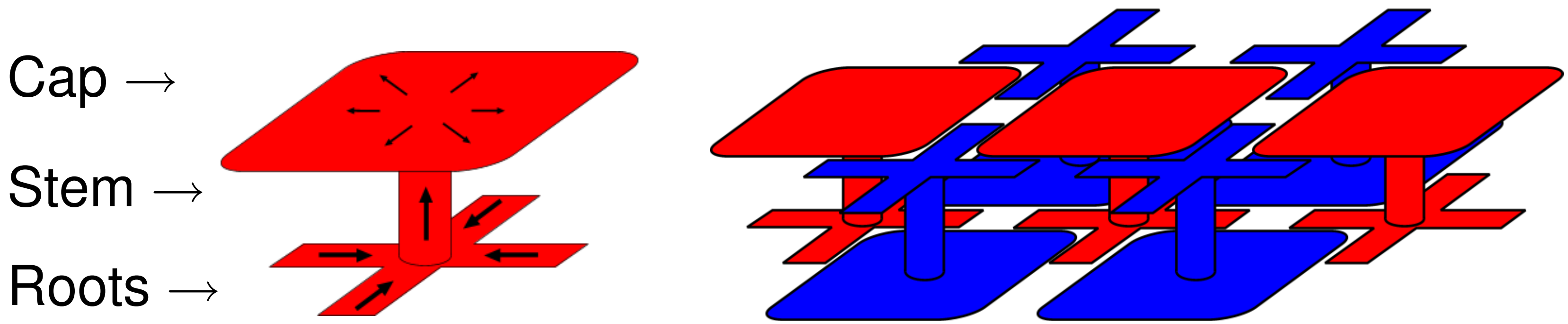

Outline

1. DNS and LES of turbulent Rayleigh–Bénard convection in wide cylindrical containers
2. Dependences of the flow patterns on Ra and Γ
3. Thermal plume extraction
4. Thermal dissipation rate analysis
5. Spatial distribution of the local heat fluxes

Spatial distribution of the thermal dissipation rate $\varepsilon_\theta = \Gamma^{-3/2} Ra^{-1/2} Pr^{-1/2} (\nabla T)^2$

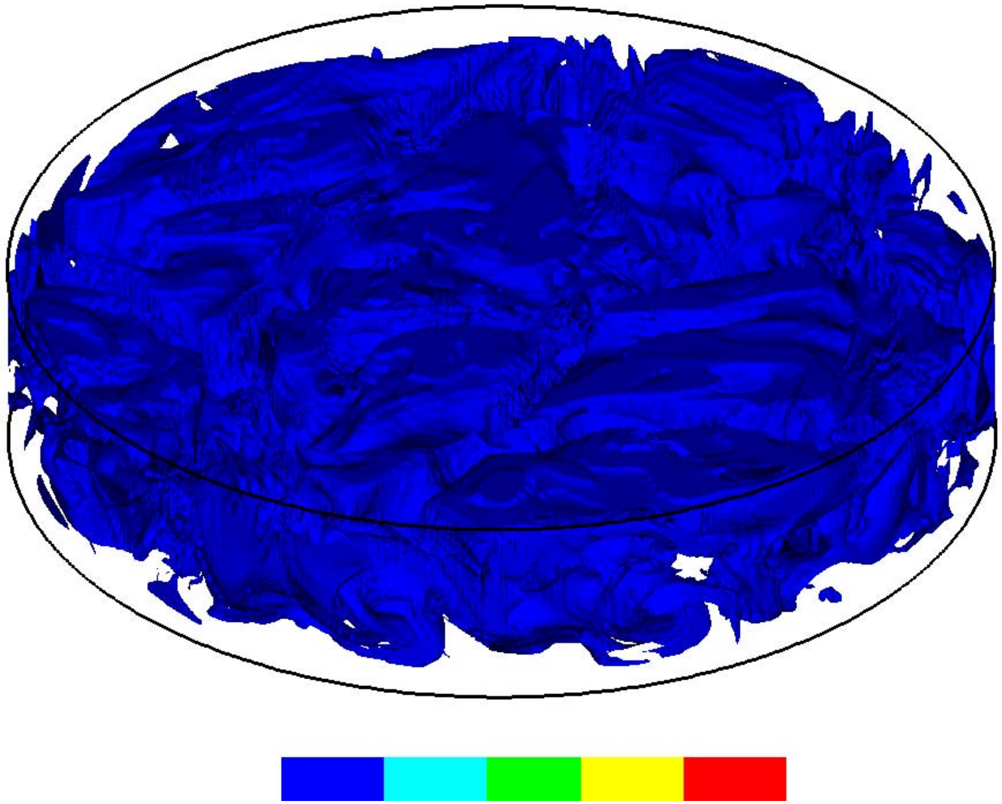

$Ra = 10^6$, $\Gamma = 5$

Deep-blue	$0 \leq \frac{\varepsilon_\theta}{\varepsilon_{\theta,\max}} \leq 5 \cdot 10^{-4}$
Blue	$5 \cdot 10^{-4} < \frac{\varepsilon_\theta}{\varepsilon_{\theta,\max}} \leq 2 \cdot 10^{-3}$
Green	$2 \cdot 10^{-3} < \frac{\varepsilon_\theta}{\varepsilon_{\theta,\max}} \leq 3 \cdot 10^{-3}$
Yellow	$3 \cdot 10^{-3} < \frac{\varepsilon_\theta}{\varepsilon_{\theta,\max}} \leq 5 \cdot 10^{-3}$
Red	$5 \cdot 10^{-3} < \frac{\varepsilon_\theta}{\varepsilon_{\theta,\max}} \leq 10^{-2}$

with $\varepsilon_{\theta,\max} = \max_V \varepsilon_\theta$

Spatial distribution of the thermal dissipation rate $\varepsilon_\theta = \Gamma^{-3/2} Ra^{-1/2} Pr^{-1/2} (\nabla T)^2$

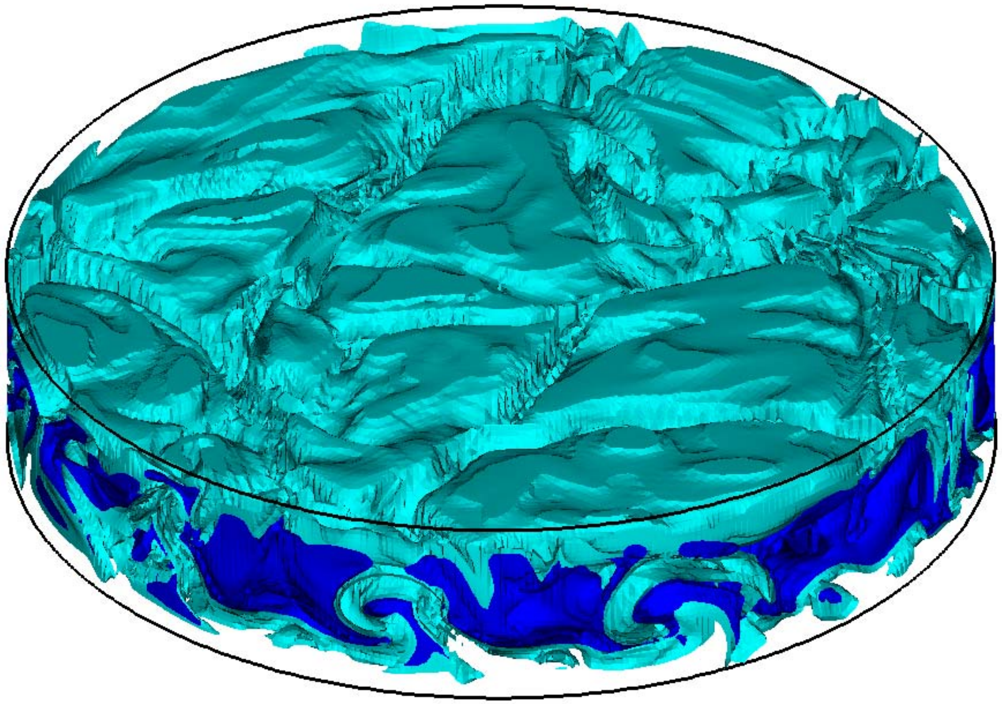

$Ra = 10^6$, $\Gamma = 5$

Deep-blue	$0 \leq \frac{\varepsilon_\theta}{\varepsilon_{\theta,\max}} \leq 5 \cdot 10^{-4}$
Blue	$5 \cdot 10^{-4} < \frac{\varepsilon_\theta}{\varepsilon_{\theta,\max}} \leq 2 \cdot 10^{-3}$
Green	$2 \cdot 10^{-3} < \frac{\varepsilon_\theta}{\varepsilon_{\theta,\max}} \leq 3 \cdot 10^{-3}$
Yellow	$3 \cdot 10^{-3} < \frac{\varepsilon_\theta}{\varepsilon_{\theta,\max}} \leq 5 \cdot 10^{-3}$
Red	$5 \cdot 10^{-3} < \frac{\varepsilon_\theta}{\varepsilon_{\theta,\max}} \leq 10^{-2}$

with $\varepsilon_{\theta,\max} = \max_V \varepsilon_\theta$

Spatial distribution of the thermal dissipation rate $\varepsilon_\theta = \Gamma^{-3/2} Ra^{-1/2} Pr^{-1/2} (\nabla T)^2$

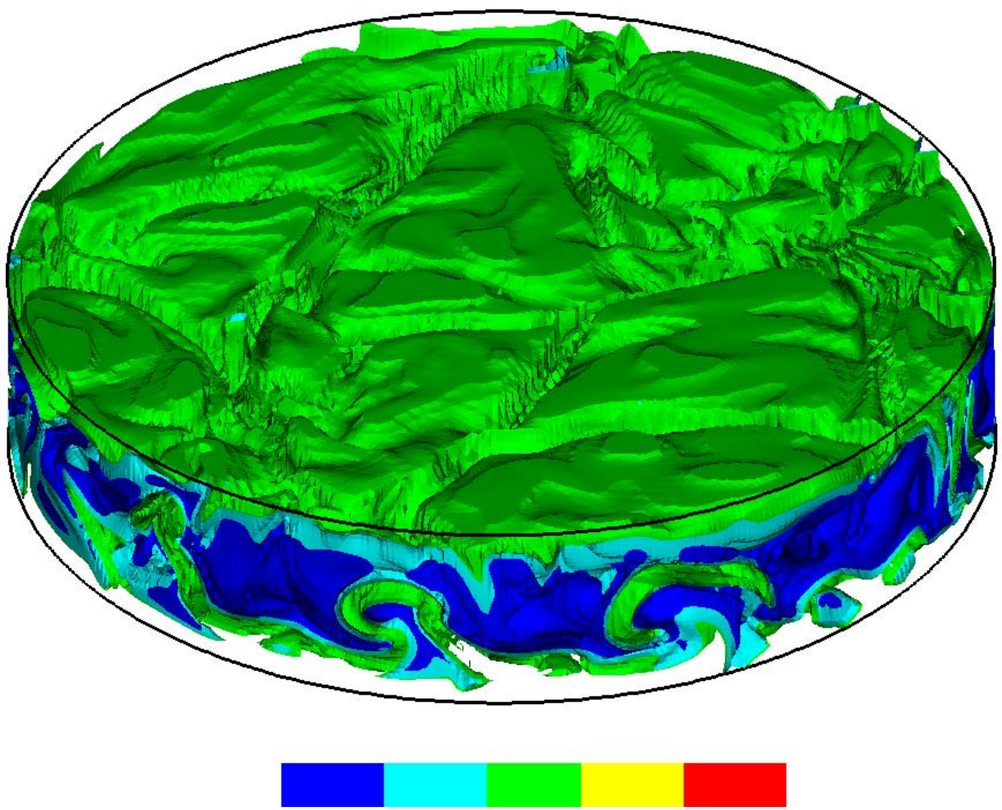

$Ra = 10^6$, $\Gamma = 5$

Deep-blue $0 \le \frac{\varepsilon_\theta}{\varepsilon_{\theta,\mathrm{max}}} \le 5 \cdot 10^{-4}$

Blue $5 \cdot 10^{-4} < \frac{\varepsilon_\theta}{\varepsilon_{\theta,\mathrm{max}}} \le 2 \cdot 10^{-3}$

Green $2 \cdot 10^{-3} < \frac{\varepsilon_\theta}{\varepsilon_{\theta,\mathrm{max}}} \le 3 \cdot 10^{-3}$

Yellow $3 \cdot 10^{-3} < \frac{\varepsilon_\theta}{\varepsilon_{\theta,\mathrm{max}}} \le 5 \cdot 10^{-3}$

Red $5 \cdot 10^{-3} < \frac{\varepsilon_\theta}{\varepsilon_{\theta,\mathrm{max}}} \le 10^{-2}$

with $\varepsilon_{\theta,\mathrm{max}} = \max_V \varepsilon_\theta$

Spatial distribution of the thermal dissipation rate $\varepsilon_\theta = \Gamma^{-3/2} Ra^{-1/2} Pr^{-1/2} (\nabla T)^2$

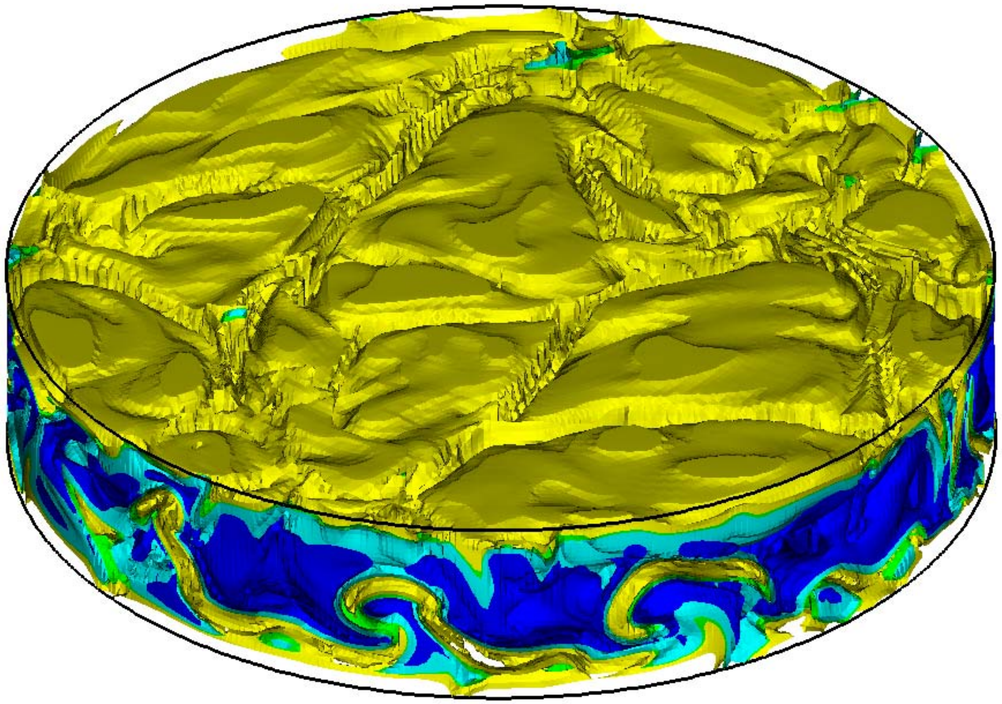

$Ra = 10^6$, $\Gamma = 5$

Deep-blue	$0 \le \frac{\varepsilon_\theta}{\varepsilon_{\theta,\max}} \le 5 \cdot 10^{-4}$
Blue	$5 \cdot 10^{-4} < \frac{\varepsilon_\theta}{\varepsilon_{\theta,\max}} \le 2 \cdot 10^{-3}$
Green	$2 \cdot 10^{-3} < \frac{\varepsilon_\theta}{\varepsilon_{\theta,\max}} \le 3 \cdot 10^{-3}$
Yellow	$3 \cdot 10^{-3} < \frac{\varepsilon_\theta}{\varepsilon_{\theta,\max}} \le 5 \cdot 10^{-3}$
Red	$5 \cdot 10^{-3} < \frac{\varepsilon_\theta}{\varepsilon_{\theta,\max}} \le 10^{-2}$

with $\varepsilon_{\theta,\max} = \max_V \varepsilon_\theta$

Spatial distribution of the thermal dissipation rate $\varepsilon_\theta = \Gamma^{-3/2} Ra^{-1/2} Pr^{-1/2} (\nabla T)^2$

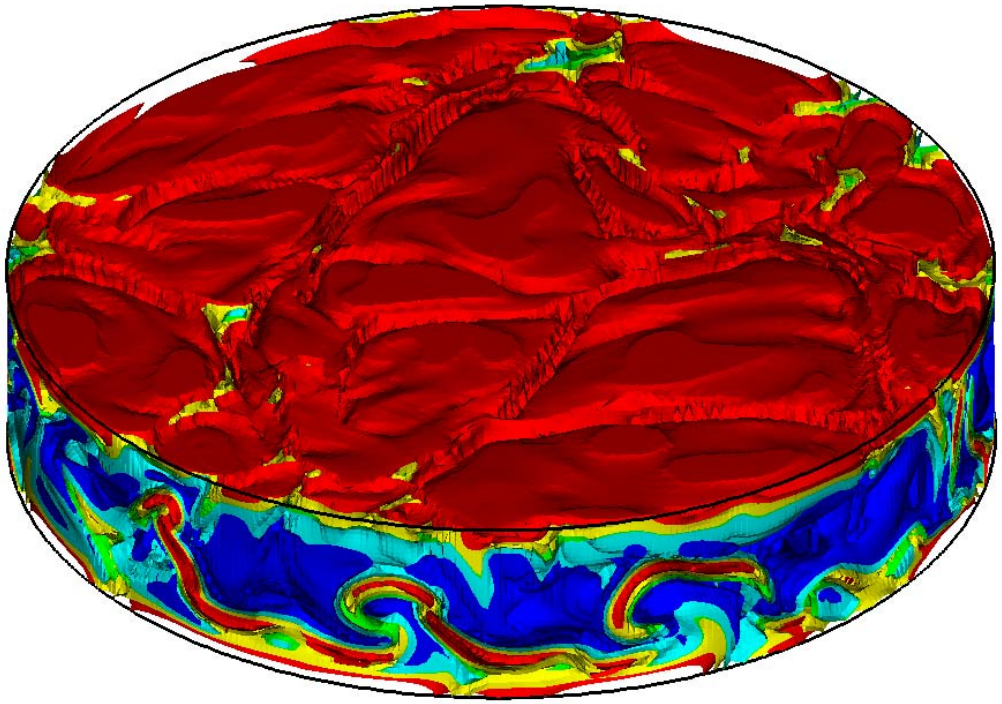

$Ra = 10^6$, $\Gamma = 5$

Deep-blue $0 \leq \frac{\varepsilon_\theta}{\varepsilon_{\theta,\max}} \leq 5 \cdot 10^{-4}$

Blue $5 \cdot 10^{-4} < \frac{\varepsilon_\theta}{\varepsilon_{\theta,\max}} \leq 2 \cdot 10^{-3}$

Green $2 \cdot 10^{-3} < \frac{\varepsilon_\theta}{\varepsilon_{\theta,\max}} \leq 3 \cdot 10^{-3}$

Yellow $3 \cdot 10^{-3} < \frac{\varepsilon_\theta}{\varepsilon_{\theta,\max}} \leq 5 \cdot 10^{-3}$

Red $5 \cdot 10^{-3} < \frac{\varepsilon_\theta}{\varepsilon_{\theta,\max}} \leq 10^{-2}$

with $\varepsilon_{\theta,\max} = \max_V \varepsilon_\theta$

Contribution to $\langle \varepsilon_\theta \rangle_V$ from the subdomain $\varepsilon_\theta \le \xi \varepsilon_{\theta,\mathrm{max}}$

$$\sigma(\xi) = \frac{\langle \varepsilon_\theta \vartheta(\xi \varepsilon_{\theta,\mathrm{max}} - \varepsilon_\theta) \rangle_V}{\langle \varepsilon_\theta \rangle_V},$$

with $\vartheta(x)$ – the Heaviside function

Contribution to $\langle \varepsilon_\theta \rangle_V$ from the subdomain $\varepsilon_\theta \leq \xi \varepsilon_{\theta,\mathrm{max}}$

$$\sigma(\xi) = \frac{\langle \varepsilon_\theta \vartheta(\xi \varepsilon_{\theta,\mathrm{max}} - \varepsilon_\theta) \rangle_V}{\langle \varepsilon_\theta \rangle_V},$$

with $\vartheta(x)$ – the Heaviside function

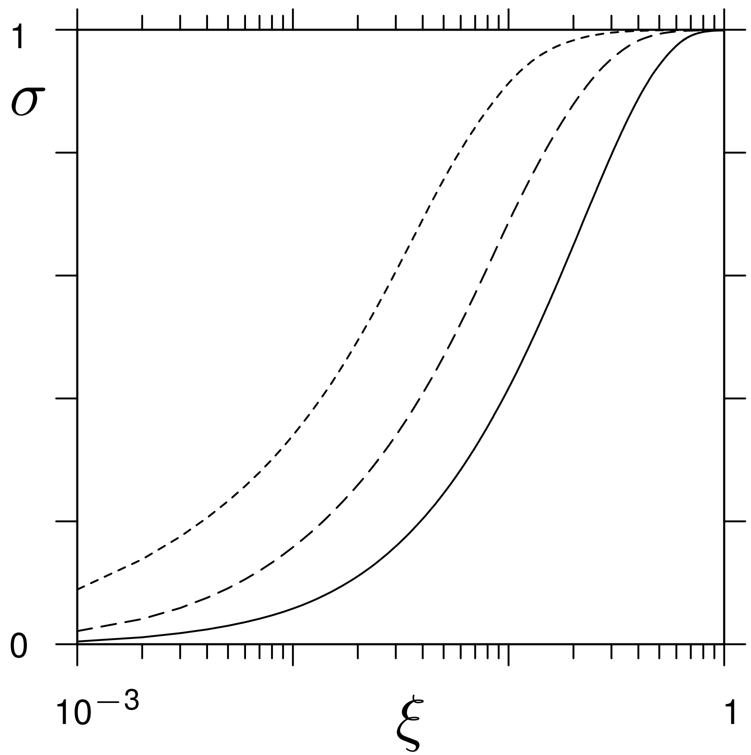

For $\Gamma = 10$ the parts of the domain, where ε_θ is less than 0.1% of its maximum, contribute

- 0.4% ($Ra = 10^5$, ——)
- 2.1% ($Ra = 10^6$, – – –)
- 8.9% ($Ra = 10^7$, - - - -)

to the volume averaged $\langle \varepsilon_\theta \rangle_V$.

Contribution to $\langle \varepsilon_\theta \rangle_V$ from the subdomain $\varepsilon_\theta \leq \xi \varepsilon_{\theta,\max}$

$$\sigma(\xi) = \frac{\langle \varepsilon_\theta \vartheta(\xi \varepsilon_{\theta,\max} - \varepsilon_\theta) \rangle_V}{\langle \varepsilon_\theta \rangle_V},$$

with $\vartheta(x)$ – the Heaviside function

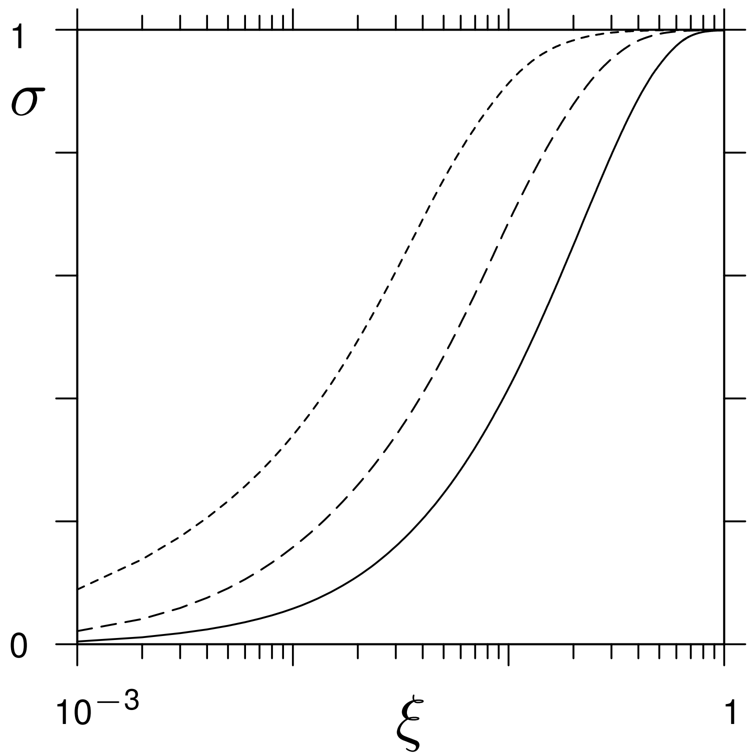

The turbulent background part of the volume averaged thermal dissipation rate increases with the Rayleigh number.

Contribution to $\langle \varepsilon_\theta \rangle_V = \Gamma^{1/2} Ra^{-1/2} Pr^{-1/2} Nu$ with growing Ra

Turbulent background

$\Uparrow$

- Grossmann & Lohse **407** *JFM* (2000)
- Shishkina & Wagner **546** *JFM* (2006)

Contribution to $\langle \varepsilon_\theta \rangle_V = \Gamma^{1/2} Ra^{-1/2} Pr^{-1/2} Nu$ with growing *Ra*

Boundary layers

$\uparrow$

Turbulent background

$\uparrow$

- Grossmann & Lohse **407** *JFM* (2000)
- Shishkina & Wagner **546** *JFM* (2006)
- Verzicco & Camussi **477** *JFM* (2003)

Contribution to $\langle \varepsilon_\theta \rangle_V = \Gamma^{1/2} Ra^{-1/2} Pr^{-1/2} Nu$ with growing *Ra*

Boundary layers

↑

Thermal plumes

↓

Turbulent background

↑

Contribution of the thermal plumes decreases with growing *Ra*

Outline

1. DNS and LES of turbulent Rayleigh–Bénard convection in wide cylindrical containers
2. Dependences of the flow patterns on Ra and Γ
3. Thermal plume extraction
4. Thermal dissipation rate analysis
5. Spatial distribution of the local heat fluxes

Local heat flux Ω for $Ra = 10^6$, $\Gamma = 5$

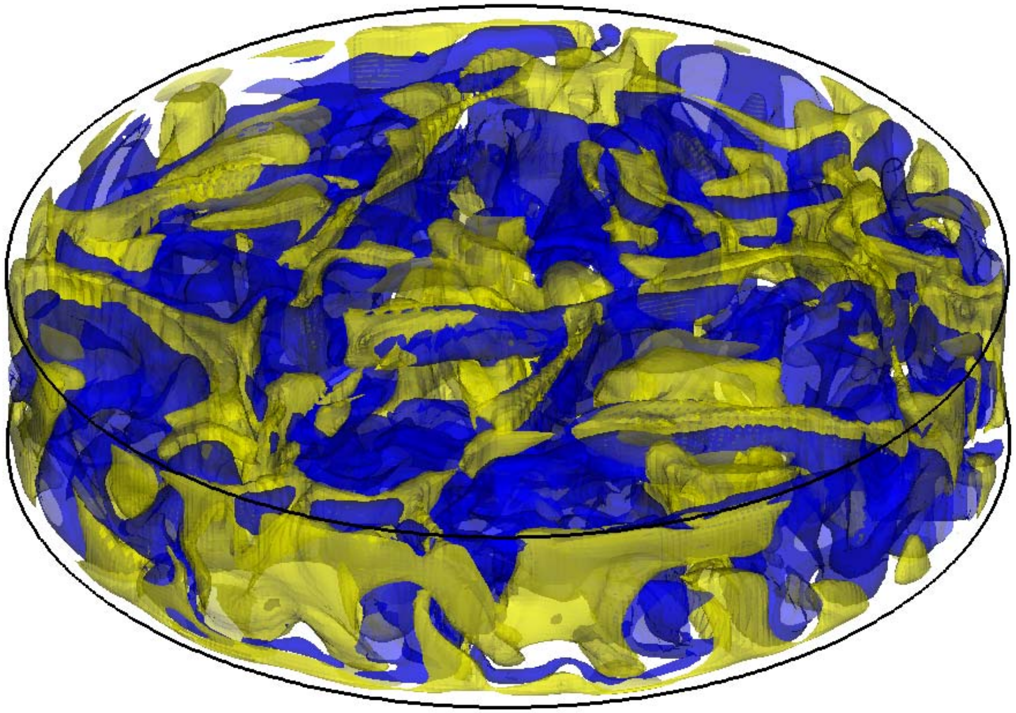

Blue $\Omega < 0$

Yellow $\Omega \geq 2Nu$

Up to 1/3 of the Rayleigh cell corresponds to negative Ω

Local heat flux Ω for $Ra = 10^8$, $\Gamma = 5$

$z = 10^{-3}H$

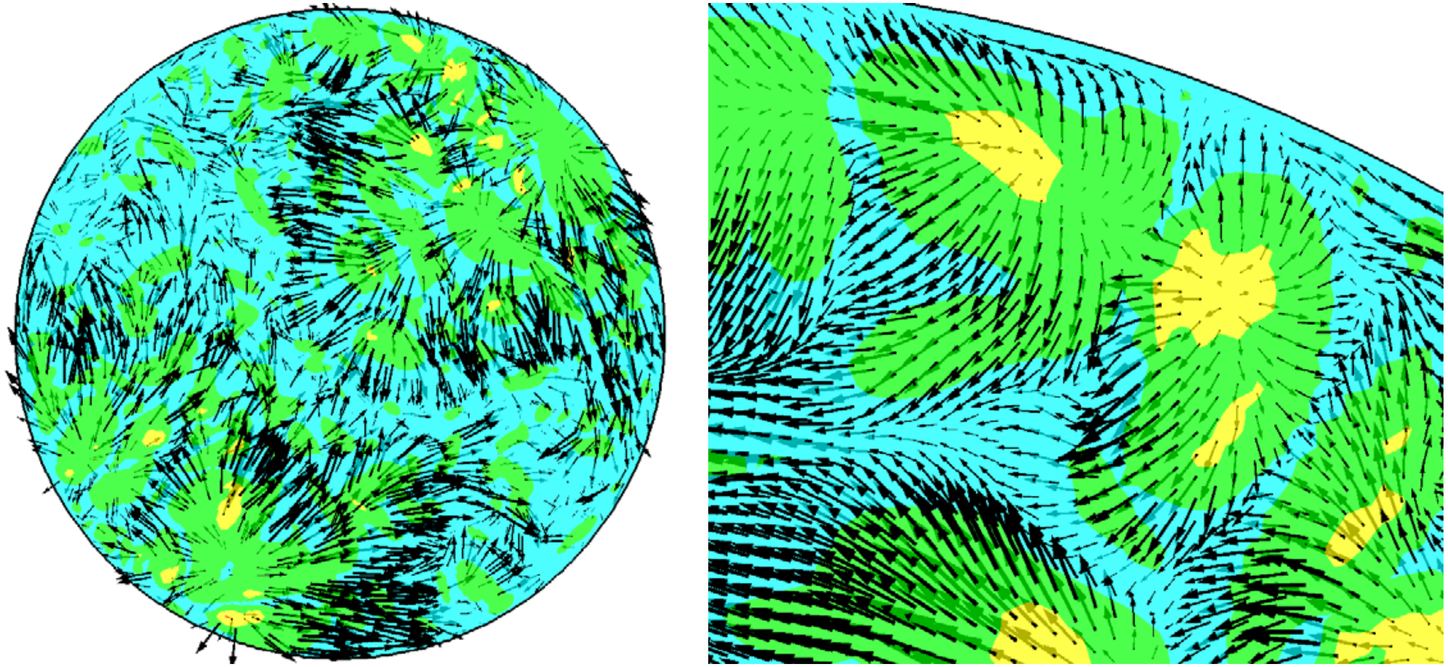

Regions of high Ω-values correspond to the thermal plumes

Local heat flux Ω for $Ra = 10^8$, $\Gamma = 5$

$z = H/2$

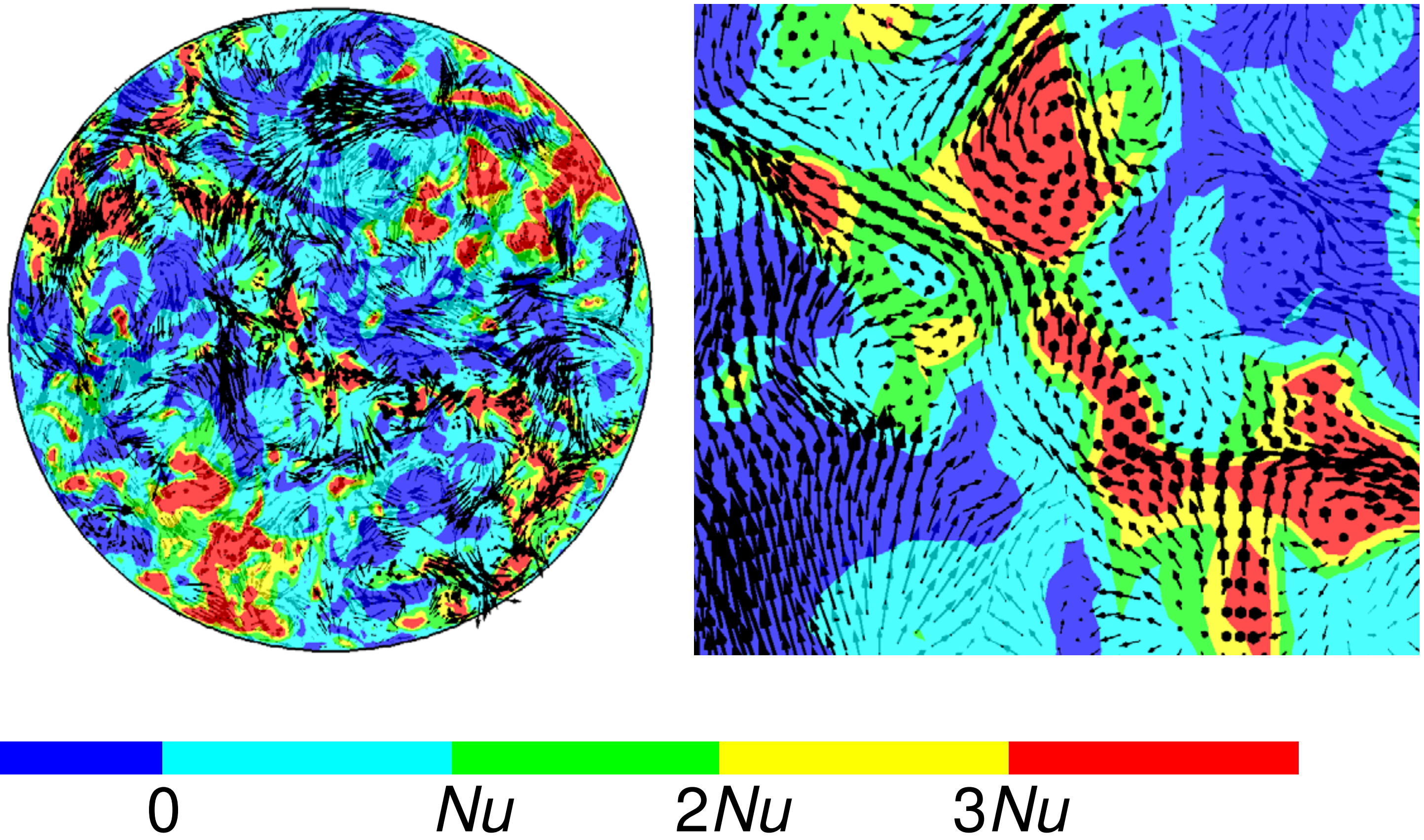

Spectrum of Ω-values widens while moving away from the plates

Mean heat flux $< \Omega >_{t,\varphi}$ near the vertical wall

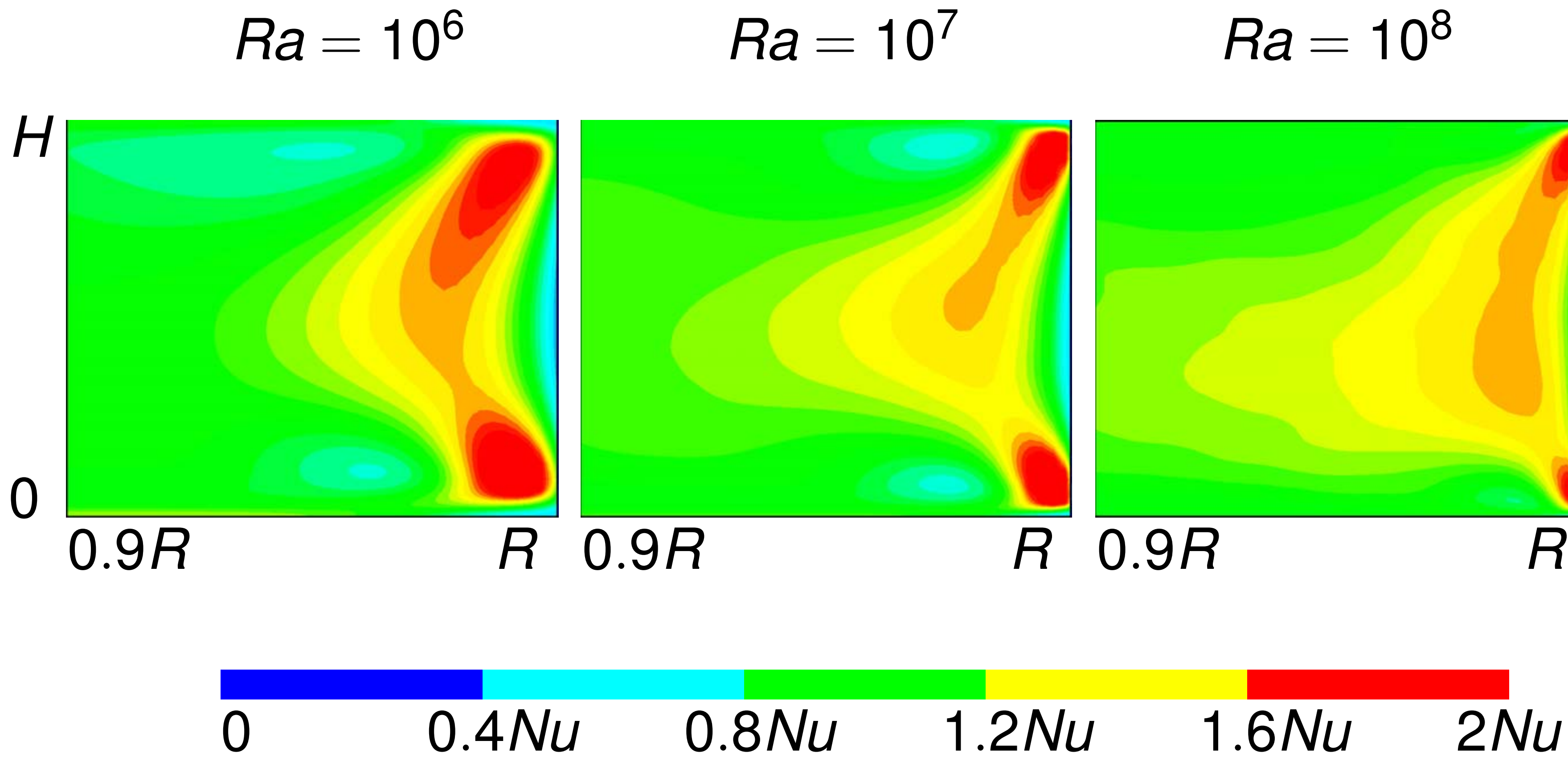

With growing *Ra* maximum points move closer to the corners

Mean heat flux $< \Omega >_{t,\varphi}$ near the vertical wall

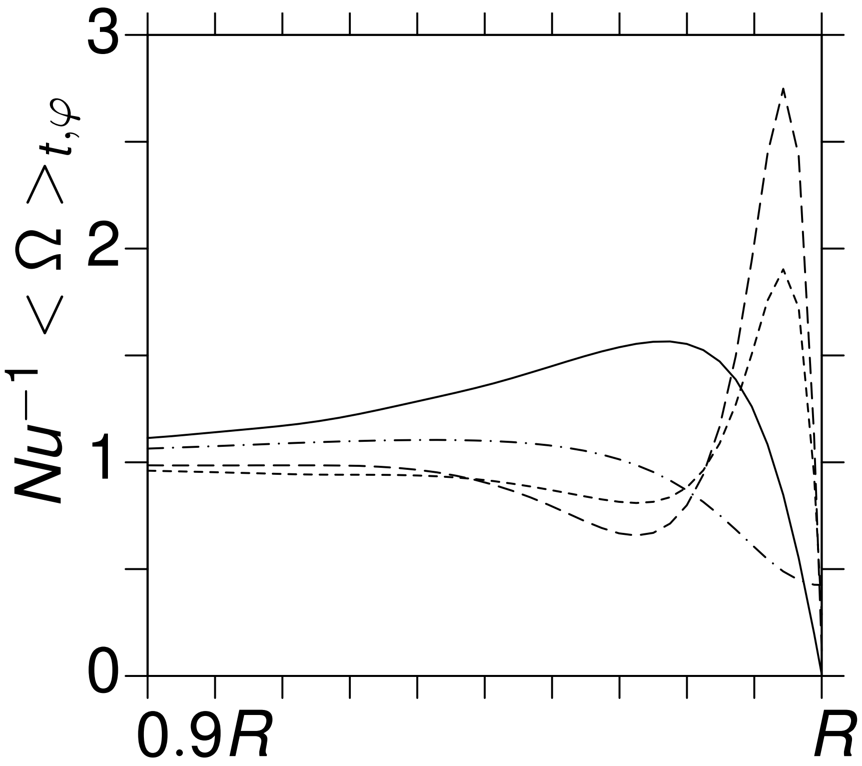

The case $Ra = 10^7$

- ——— $z = H/2$
- – – – $z = H/(Nu)$
- - - - - $z = H/(2Nu)$
- – · – $z = 10^{-3}H$

Highest values of $< \Omega >_{t,\varphi}$ are approached in the bulk at distance $z \approx Nu^{-1}H$ from the horizontal plates

DLR

Density functions of the temperature and axial velocity

for $Ra = 10^8$ (——), $Ra = 10^7$ (– – –) and $Ra = 10^6$ (- - - -)

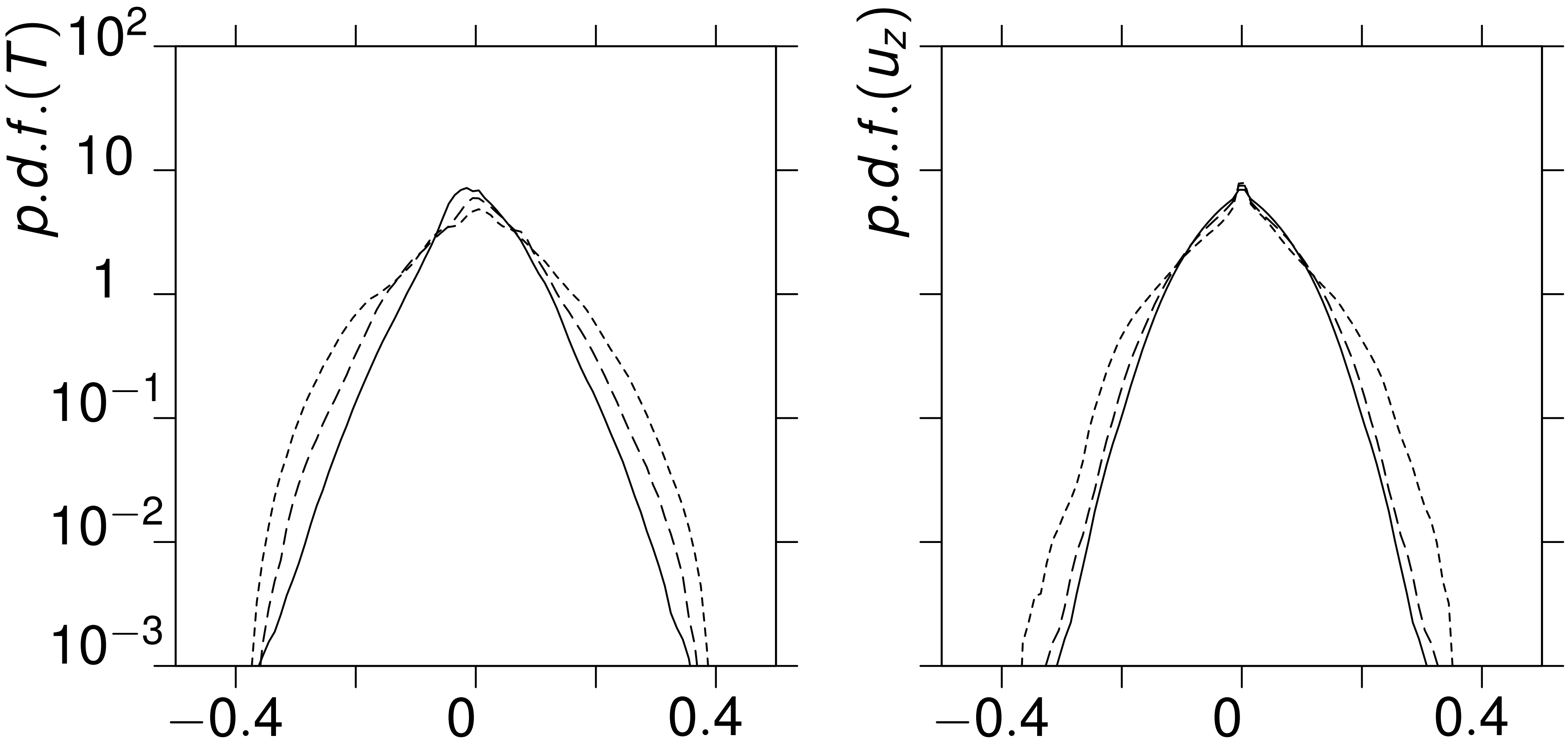

p.d.f. of T and u_z are symmetric

Volume distribution density function of the heat flux Ω

for $Ra = 10^8$ (——), $Ra = 10^7$ (– – –) and $Ra = 10^6$ (- - - -), $\Gamma = 5$, $\delta = 0.08$

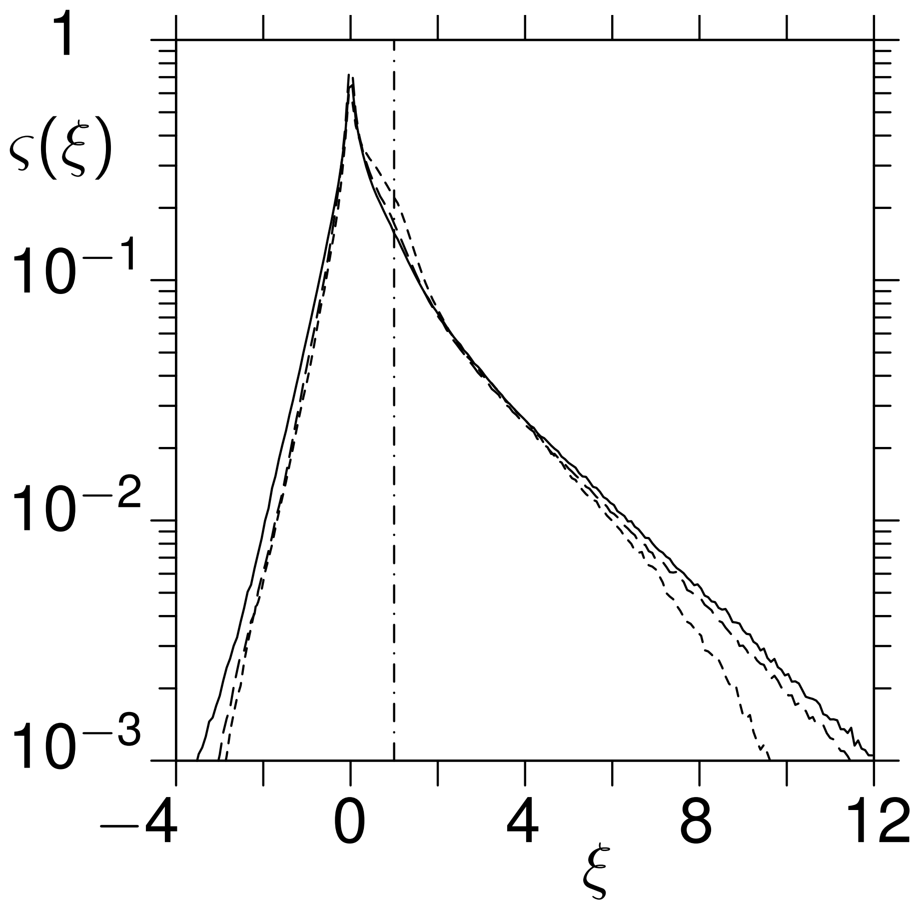

$$\varsigma(\xi) = \frac{1}{\delta}\left\langle \vartheta\left(\Omega - (\xi_i - \frac{\delta}{2})Nu\right)\right\rangle_V - \frac{1}{\delta}\left\langle \vartheta\left(\Omega - (\xi_i + \frac{\delta}{2})Nu\right)\right\rangle_V$$

with the Heaviside function

$$\vartheta(x) = \begin{cases} 1, & \text{if } x \geq 0, \\ 0, & \text{otherwise,} \end{cases}$$

and integer $(\xi_i/\delta + 1/2)$

Volume distribution density function of the heat flux Ω

for $Ra = 10^8$ (——), $Ra = 10^7$ (– – –) and $Ra = 10^6$ (- - - -), $\Gamma = 5$, $\delta = 0.08$

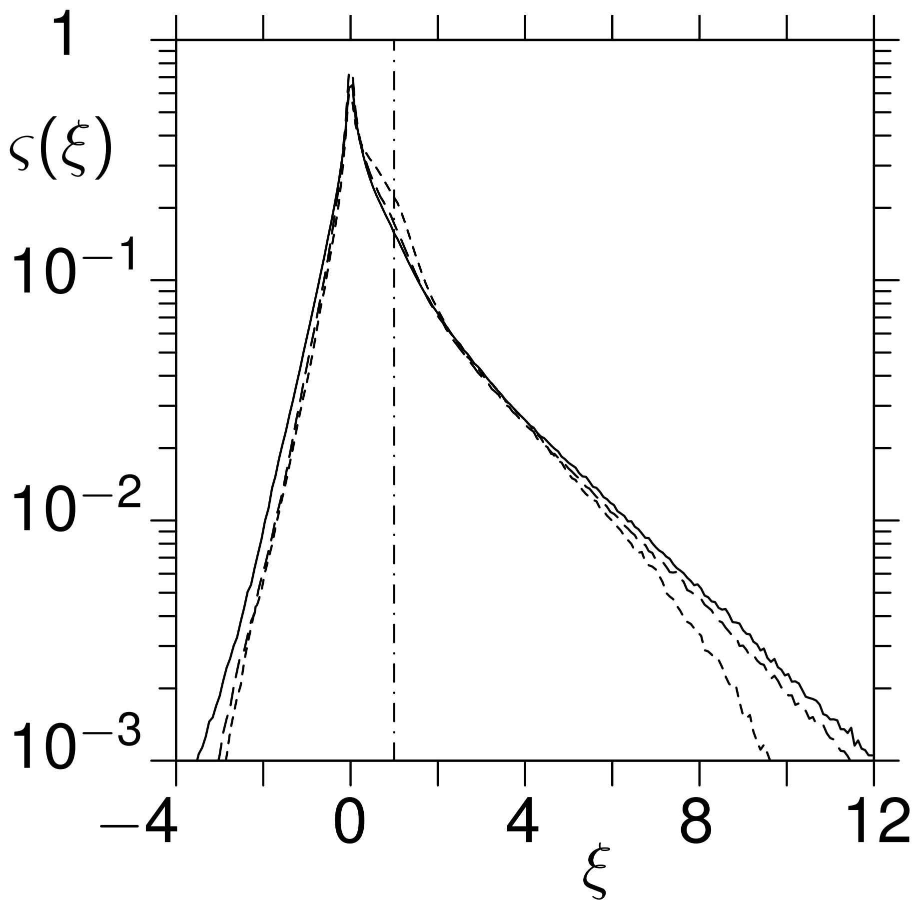

$\varsigma(\xi)$ for $\xi \in [\xi_i - \frac{\delta}{2}, \xi_i + \frac{\delta}{2}[$ indicates the percentage of the fluid volume with $\Omega \in [(\xi_i - \frac{\delta}{2})Nu, (\xi_i + \frac{\delta}{2})Nu[$

Volume distribution density function of the heat flux Ω

for $Ra = 10^8$ (——), $Ra = 10^7$ (– – –) and $Ra = 10^6$ (- - - -), $\Gamma = 5$, $\delta = 0.08$

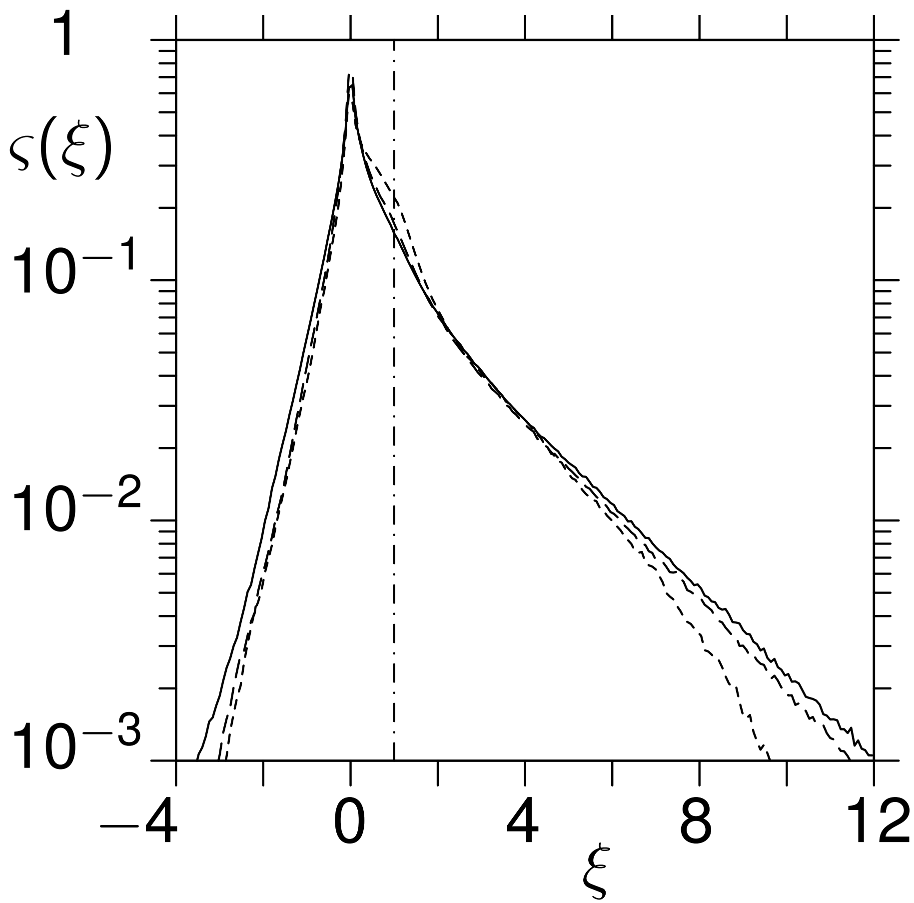

Spatial distribution of Ω

%% vs. Ra	10^6	10^7	10^8
$\Omega < 0$	25	28	31
$0 \leq \Omega < 2Nu$	58	54	51
$\Omega \geq 2Nu$	17	18	18

DLR

Areal distribution density function of the heat flux Ω

for $Ra = 10^7$, $z = 0.5H$ (——), $z = H/(2Nu)$ (– – –) and $z = 10^{-3}H$ (- - - -)

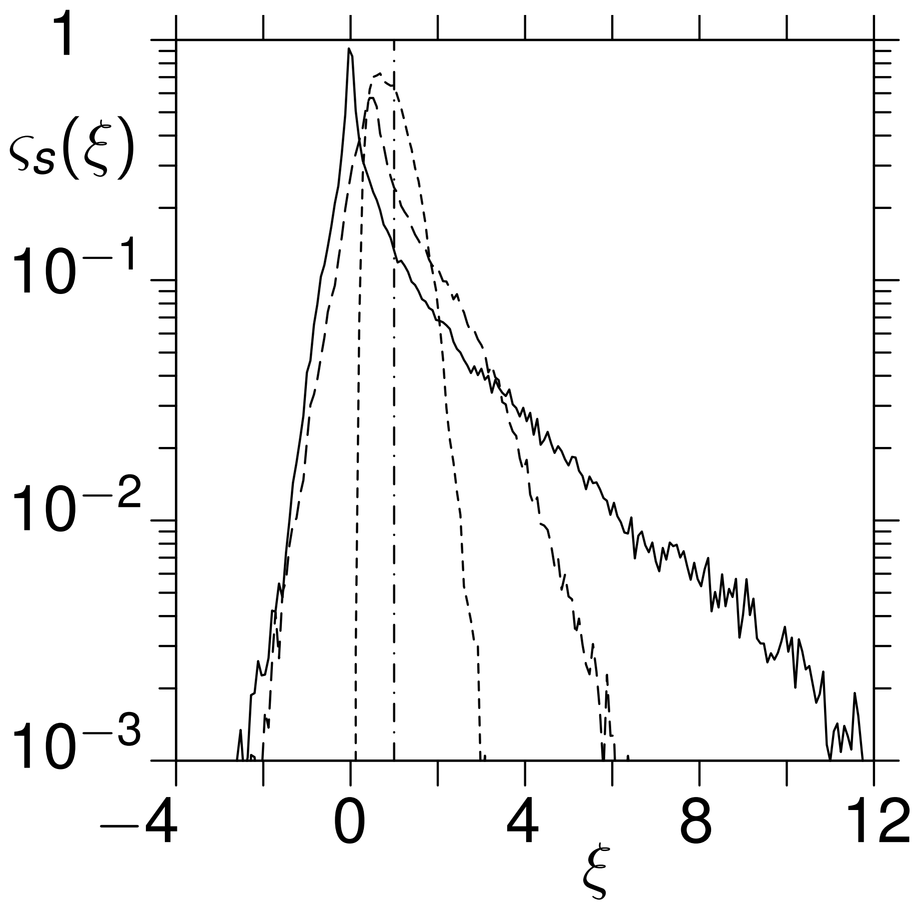

$$\varsigma_s(\xi) = \frac{1}{\delta}\left\langle \vartheta\left(\Omega - (\xi_i - \frac{\delta}{2})Nu\right)\right\rangle_{S_z} - \frac{1}{\delta}\left\langle \vartheta\left(\Omega - (\xi_i + \frac{\delta}{2})Nu\right)\right\rangle_{S_z}$$

indicates the portion of S_z with $\Omega \in [(\xi_i - \frac{\delta}{2})Nu, (\xi_i + \frac{\delta}{2})Nu[$

Areal distribution density function of the heat flux Ω

for $Ra = 10^7$, $z = 0.5H$ (——), $z = H/(2Nu)$ (– – –) and $z = 10^{-3}H$ (- - - -)

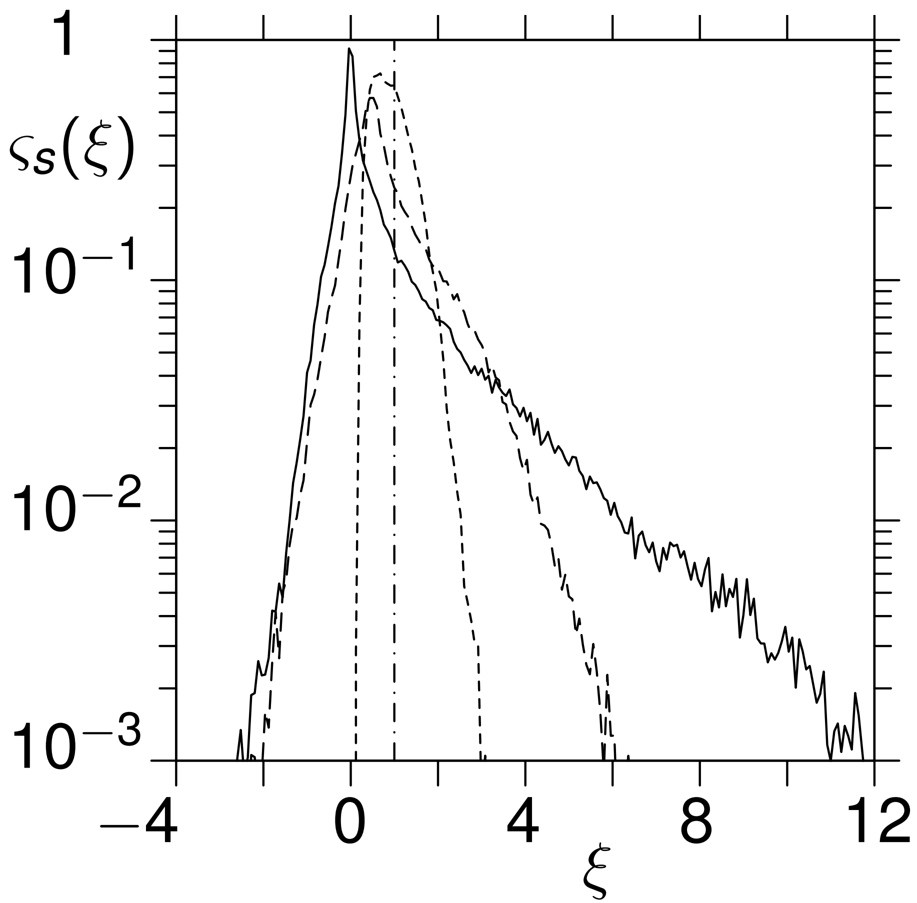

The spread of the tails in Ω-distributions widens while moving away from the plates towards the bulk

Areal distribution density function of the heat flux Ω

for $Ra = 10^7$, $z = 0.5H$ (——), $z = H/(2Nu)$ (– – –) and $z = 10^{-3}H$ (- - - -)

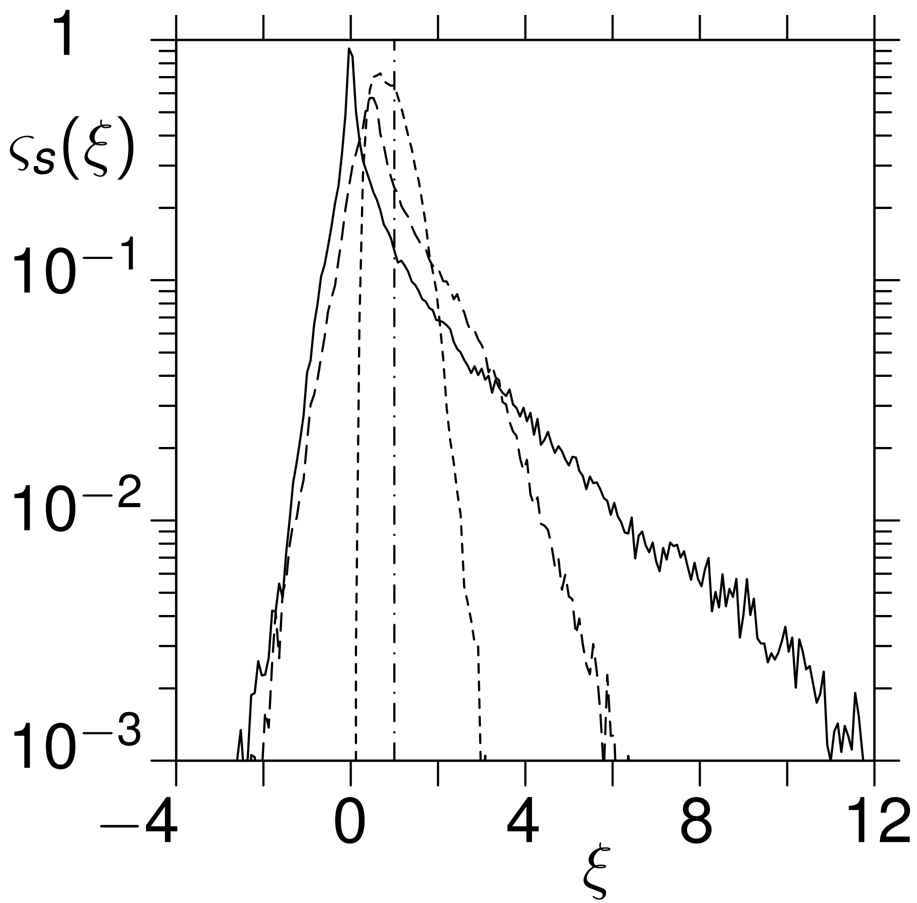

Areal distribution of Ω

%% vs. z	0	$\frac{H}{(2Nu)}$	$\frac{H}{2}$
$\Omega < 0$	0	13	31
$0 \leq \Omega < 2Nu$	98	71	50
$\Omega \geq 2Nu$	2	16	19

Main conclusions

Local heat flux Ω

The spread of the tails of the local heat flux distributions increases with the Rayleigh number and while moving away from the plates towards the bulk. Up to 1/3 of the fluid volume corresponds $\Omega < 0$. With growing *Ra* the zones of the highest values of the time-averaged local heat flux nestle closer to the corners.

Turbulent background

Both, the portion of the whole domain which corresponds to the turbulent background and the contribution to the volume averaged thermal dissipation rate from the turbulent background, increase with the Rayleigh number.